Combining microbial, isotopic and residence time data to characterize groundwater dynamics in a multi-layered aquifer system in Kurikka, western Finland

Lotta Purkamo[1], Juuso Ikonen[1], Marie-Amélie Pétré[1,2], Niko Putkinen[1], Jürgen Sültenfuss[3], Minna Myllyperkiö[1], Anna-Maria Hokajärvi[4], Tarja Pitkänen[4,5], Ilkka T. Miettinen[4]

[1]Geological Survey of Finland (GTK), Espoo, 02150, Finland
[2]BRGM (French Geological Survey), 3 Avenue Claude Guillemin, Orléans 45100, France
[3]University of Bremen, Otto Hahn Allee 1, 28359 Bremen, Germany
[4]Finnish Institute for Health and Welfare (THL), Department of Public Health, Kuopio, 70210, Finland
[5]University of Helsinki, Faculty of Veterinary Medicine, Helsinki, 00014, Finland

Correspondence to: Lotta Purkamo (lotta.purkamo@gtk.fi)

Abstract. Groundwater is a critical resource supplying nearly half of the world's drinking water. This study focuses on the Kurikka buried valley aquifer system in western Finland, characterized by complex hydrogeology dictated by the bedrock topography and sediment cover producing artesian conditions in deep aquifers. Using a multitracer approach, the study incorporates hydrogeochemical, isotopic ($\delta^{34}S$, $^{87}Sr/^{86}Sr$) and microbial community analyses with residence time indicators (CFCs, SF_6, ^3H, $^3H/^3He$). Groundwater samples collected from ten sites revealed differences in residence times, microbial diversity and community compositions, as well as large variation in the strontium and sulphur isotopic compositions. The bedrock groundwater sample revealed a more evolved water type, consistent with longer residence time, strong water-mineral interactions and typical deep subsurface bacterial members. Groundwater from the superficial unconsolidated aquifers contained a modern water component (<60 years) whereas the deeper buried valley aquifers were characterized by older waters. The information provided by this study is crucial for groundwater management during extensive extraction for municipal water supply.

1 Introduction

Groundwater provides an essential water supply worldwide. Almost half of all drinking water globally, 65 - 75% in Europe (27 EU Member States) and 38% in the US (Grönwall and Danert 2020, Johnson et al. 2022, National Ground Water Association) originates from groundwater. In Finland, approximately 60% of water distributed by waterworks is groundwater and the management of groundwater resources is crucial to the success of the water utilities producing good quality drinking water (Kløve et al. 2017). To manage the groundwater resources sustainably, a significant understanding of the aquifer is essential. Hydrogeochemical studies are a key factor in understanding the functioning of hydrogeological systems, including groundwater origin, flow path, residence time, mixing, and the processes affecting the groundwater quality in an aquifer. While

multitracer approaches commonly involve major, minor, and trace elements, stable water isotopes, and environmental tracers used to assess groundwater residence times, this study aims to go further by incorporating microbial community analyses along with strontium and sulphur isotopes. Previous studies have shown the potential usability of microbial community analysis in hydrogeological studies (Ben Maamar et al. 2015). Here we show that microbial data can provide novel insights into aquifer functioning within a buried valley aquifer system in western Finland, hosting significant water resources. This study is part of a larger hydrogeological research initiative, incorporating hydrogeological and geological modelling with extensive hydrogeochemical characterization of the flow system, in which the main goal is to find enough groundwater to support large-scale abstraction to meet the water demands of 150,000 residents and the industries in cities of Vaasa and Kurikka. The goal of this study was to determine the baseline information on the hydrogeochemical and microbiological properties that enable the monitoring of the evolution of the water system during operational stage. The aquifer system has a complex groundwater recharge route originating from the high-standing areas west of the Kurikka buried valleys. From the recharge area, groundwater flows toward the buried valley aquifers, where a coarse-grained aquifer consists of the interplay between permeable sediments and fractured crystalline bedrock (Putkinen et al. in review 2025, Åberg et al. 2026). However, the flow paths and potential mixing of shallow and deeper groundwater, including possible input from the deep bedrock groundwater, are still poorly understood.

Hydrogen ($\delta^{2}H$) and oxygen ($\delta^{18}O$) isotopic composition of the water molecule can be used together with the isotopic compositions of selected solutes in the water sample to characterize water types, trace the origin of the water and assess mixing of different waters and water pathways, as well as to extract more information on the chemical and biological processes in the study area (Carreira and Marques 2024, Ikonen et al. 2025, Luoma et al. 2024, Porru et al. 2024, Åberg et al. 2025). Changes in the isotopic compositions during the water cycle, from precipitation to groundwater recharge and eventual discharge, produce the tracer characteristics and form the basis for using isotopes as tracers in hydrogeological studies. With oxygen and hydrogen, the fractionation is caused by physical processes, i.e. evaporation, or mixing of different waters. The aim here was to use the water stable isotopes to determine the origin of water and residence times of the groundwater samples from the deep unconsolidated aquifer and the bedrock observation well and to assess the recharge periods for the groundwater.

Strontium (Sr) has four stable isotopes ^{88}Sr (82.53 %), ^{87}Sr (7.04 %), ^{86}Sr (9.87 %), and ^{84}Sr (0.56 %). As a result of radioactive decay of rubidium, the amount of the radiogenic isotope ^{87}Sr increases over geologic time. The stable and constant ^{86}Sr is used to determine the $^{87}Sr/^{86}Sr$ ratio that is commonly used in hydrogeological studies (Shand et al. 2009). The isotopic composition of strontium analysed from a water sample corresponds to the local geochemistry. In Finland, the mineralogy of rock types usually produces an $^{87}Sr/^{86}Sr$ value between 0.7 – 0.8 (Kaislaniemi 2011). The silicate-rich rocks have higher potassium content (potassium feldspar, mica minerals) producing the higher $^{87}Sr/^{86}Sr$ values, while carbonate rocks rich in calcium are associated with lower $^{87}Sr/^{86}Sr$ values closer to the $^{87}Sr/^{86}Sr$ value of seawater (0.709). The isotopic composition of strontium can be characterized as a conservative tracer, since there is no noticeable fractionation in chemical or biological reactions in low

temperature/pressure environments (Bullen et al. 1996, Shand et al. 2009). Isotopic analysis of strontium was selected here to reveal information on the local mineralogy, and to see if information on groundwater mixing could be revealed and to set a precursor for further isotopic studies in the area.

The isotopic composition of sulphur (S), represented as $\delta^{34}S$, is the deviation of the ratio of its two isotopes ^{32}S and ^{34}S from the international standard. The range of the isotopic composition of sulphur is normally explained by the sulphur source material (i.e. sulphide minerals), variation in redox conditions and microbial activity. The most important fractionation process in low temperature unconsolidated environments is the microbial reduction of sulphur, where microbes facilitate the removal of the lighter ^{32}S, increasing the ratio in the dissolved sulphur of the water sample (Onac et al. 2011). Sulphide oxidation (reoxidation), in turn, produces lighter isotopic compositions of sulphur in water samples. The isotopic composition of sulphur from a water sample can be linked to the microbiological data (Harrison and Thode 1958, Kaplan and Rittenberg 1963. Samborska-Goik and Bottrell, 2025). Enzymes needed for sulphate reduction process work more efficiently on breaking break the ^{32}S-O bond that produces the enrichment of heavier isotope seen in the analysed water. The analysis of $\delta^{34}S$ was used in this study to link the microbial communities to the isotopic compositions of sulphur in the groundwater samples.

As part of this multitracer approach, several groundwater residence time indicators were used to characterize the buried valley aquifer system: Tritium (^{3}H), chlorofluorocarbons (CFCs), sulphur hexafluoride (SF_6) and noble gases (Helium isotopes and Neon). These tracers are useful because of their known input histories or predictable decay or accumulation in the subsurface. While ^{4}He is useful for dating ancient groundwater, ^{3}H, ^{3}He, CFCs and SF_6 are used to identify "modern" groundwater (typically less than 60 years old). They are used to trace groundwater flow paths and inform on the renewal rate and vulnerability of the resource, which are important in a perspective of sustainably developing the resource. These groundwater dating tools have been widely applied across a range of hydrogeological contexts, including in hard-rock aquifers (Cook and Solomon 1997; Jaunat et al. 2012; Visser et al. 2013; Åkesson et al. 2015; Meyzonnat et al. 2023, Osenbrück et al. 2006; Massmann et al. 2008, Mayer et al. 2014). An overview of the tracers for young groundwater is given in Solomon and Gilmore (2024).

Groundwater as a dark and often oligotrophic environment with relatively stable temperature selects specific microbial communities compared to the aquatic ecosystems aboveground (Lee et al., 2018). Groundwater habitats vary in geological, chemical and hydrological properties. They can cover a small water body or an entire regional aquifer spanning hundreds of kilometres. The geochemistry of the aquifer may give clues on ongoing microbial metabolic processes, but because of the enormous versatility of still unknown microbes inhabiting groundwater systems, it should not be the only source of information (Flynn et al., 2013). Understanding the microbial contribution to ecosystem processes, such as cycling of nutrients and regulating the redox environment, will aid in interpreting the biogeochemical properties of aquifers. Microbes in nutrient-poor environments are considered to represent heterotrophs that are adapted to prevailing conditions. Heterotrophs break down organic matter and release CO_2 into groundwater. On the other hand, chemolithoautotrophic organisms can be another

component of the microbial community, and their significance especially in deeper groundwater habitats is prevalent (Hutchins et al. 2016). These autotrophs can use CO_2 to produce methane in anaerobic conditions. Oxygen availability and pH play a significant role on sulphur and iron cycling as well. Sulphate and iron reduction typically require anoxic conditions, but if oxygen is available, thermodynamics favour oxidation reactions over reductive processes in groundwater. In acidic conditions, iron reducers have a significant advantage over sulphate reduction (Bethke et al., 2011). As most microbes are specialized in either reductive or oxidative metabolisms rather than being capable of both, the availability of electron donors and acceptor can determine the microbial community structure to some extent.

Although modern molecular biological methods, such as massive parallel sequencing techniques have aided the environmental microbiologists in gathering information about the taxonomic and functional diversity of microbes, microbial community structure remains to be fully exploited to understand hydraulic connections in aquifers (Merino et al., 2022). The aim of this study was to evaluate the potential of using microbial community structure, i.e. a microbial fingerprint in characterizing the groundwater ecosystem in different locations of the buried valley aquifers. Furthermore, the aim was to evaluate the applicability and compatibility of hydrochemical and isotopic tracers for aquifer characterization and apply groundwater residence time indicators to bedrock and buried valley aquifer samples to trace the origin and age of groundwater in a complex aquifer system. We hypothesize that this multitracer approach in hydrogeochemistry combined with lesser used microbial community analysis provides a tool for assessing and identifying the connectivity and flow dynamics within complex multi-aquifer systems. This information aids in making informed decisions about groundwater management.

1.1 Site description

The study site is situated in the Southern Osthrobothnia region in western Finland, 70 kilometres from the Bothnian Sea shore (Fig. 1). The groundwater system of the Kurikka buried valley is underlain by 1.88 Ga year-old Palaeoproterozoic metamorphosed granites, schists, and biotite paragneisses (Lahtinen et al. 2017, Ruuska et al. 2023). The early development of the Palaeoproterozoic bedrock during the Svecofennian orogeny with crustal movements, shaped the Kurikka area and led to the formation of protovalleys. Since then, the area has experienced a multi-stage burial-erosion development over a long period of time until it reached its current buried form (Hall et al. 2021). Currently, this ~1.5 Ga old and 70–120 m deep buried valley system is filled with highly variable Late Pleistocene sediments. In its most recent developmental stages, this region situated beneath the central sector of the Fennoscandian Ice Sheet (FIS) during the Late Weichselian Glaciation (23,000–10,500 years BP; Stroeven et al., 2016)—which covered southern Finland and facilitated the preservation of pre-existing sediments through limited glacial erosion (Putkinen et al., *in review*, 2025, Åberg et al. 2026)—remained largely unaffected. Specifically, the deepest sediments typically consist of deposits that have groundwater potential for municipal drinking water abstraction.

The regional hydrogeology of the study area (240,5 km^2, Fig.1) is strongly controlled by bedrock topography. Topographical differences, together with silt-clay sediment and basal till on the topmost part of the sediment cover, produce an artesian

character to the deep aquifers (Fig. 1). Layer cake type of stratigraphy of the buried valley with alternating aquitards and aquifers is conceptually shown in the Fig. 1, but more detailed in Åberg et al. (2026). The general direction of groundwater flow is from the highland region towards the buried valley aquifers, and it is assumed that a geochemical evolution occurs along the flow path (Putkinen et al., *in review*, 2026).

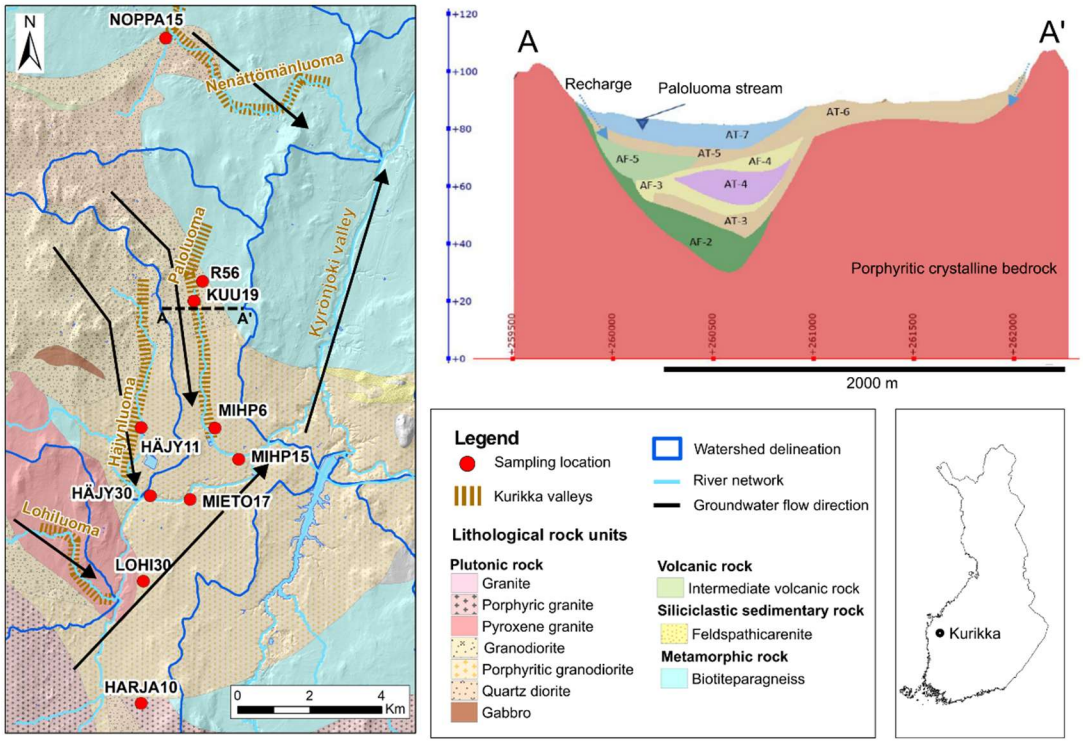

Figure 1: Left, a geological map of the study area and groundwater sampling locations; right: general cross-section of the Paloluoma buried valley (modified from Rashid 2022). Arrows in map indicate potential groundwater flow paths. AF- and AT- refer to aquifer and aquitard, respectively in the cross section. AT 3-4-5-6: till, AF3-4: fine sand, AF2: sandy gravel, AF5: coarse sand. See also Table 1. Vertical exaggeration: 15X.

2 Materials and Methods

In this multi-tracer study of the region, the sampling points were selected in each buried valley connected to the main Kyrönjoki Valley (Fig. 1). Additionally, the study included a bedrock borehole (R56) located beneath the Paloluoma valley and a point further north (NOPPA15) in an adjacent valley reflecting a more superficial esker system.

Table 1. Details of the sampling sites in Kurikka multilayer aquifer system.

Sample ID	Sampling date	Location	Total depth of the well,	Screen depth interval, m	Aquifer code[1]/type

m

NOPPA 15	4 Oct 2021	Nenättömänluoma	15.6	6.6-9.1; 10.6-13.6[2]	AF7A; Shallow unconsolidated
MIHP6	5 Oct 2021	Paloluoma	77.7	50.9-76.9	AF3A; Deep unconsolidated
MIHP15	5 Oct 2021	Paloluoma	64.6	38.1-64.6	AF3A; Deep unconsolidated
R56	5 Oct 2021	Paloluoma	162[3]	no screen[3]	Not available; Bedrock
LOHI30	5 Oct 2021	Lohiluoma	78.4	50.4-64.4	AF3A; Deep unconsolidated
KUU19	6 Oct 2021	Paloluoma	72.9	49.5-72.9	AF3A; Deep unconsolidated
HÄJY30	6 Oct 2021	Kyrönjoki main valley	17.4	no screen[4]	AF3A; Deep unconsolidated
MIETO17	6 Oct 2021	Kyrönjoki main valley	63.8	29.8-48.8; 49.8-60.8[2]	AF3A; Deep unconsolidated
HARJA10	7 Oct 2021	Kyrönjoki main valley	60.8	37.8-39.8; 41.8-51.8[2]	AF3A; Deep unconsolidated
HÄJY11	7 Oct 2021	Häjynluoma	59	39-59	AF4B; Deep unconsolidated

[1] Described in more details in Åberg et al. (2026)
[2] Two screens
[3] Bedrock borehole, no screen in the sediment layers. Total length of borehole in the table. Drilled with 60 °dip.
[4] No screen. Observation well has a total depth of 17.4 m and is open at its base. Continuously overflowing.

2.1 Field parameter measurements, geochemical and isotope sampling and analyses

The water samples were collected between 4th and 7th of October in 2021. The groundwater wells (apart from the those that were overflowing) were purged one day before sampling. The water levels were measured at non-overflowing wells before sampling. Groundwater was pumped from the wells using a submersible pump (Proactive SS-Monsoon XL, GWM Engineering, Kuopio, Finland) with pumping speed of 4-7 l/min. The field measurements for temperature (T), dissolved oxygen (DO), pH, electrical conductivity (EC) and oxygen reduction potential (ORP) were done with YSI multi-parameter sonde (YSI EXO1) (YSI Inc. Yellow Springs, OH, US). Alkalinity was measured in the field with a HACH digital titrator (HACH Company, Loveland, CO, US) and a cartridge of sulphuric acid (1.600N). The partial pressure of CO_2 (pCO_2) was

calculated with the software Diagrammes (Simler 2012) based on temperature, pH and HCO_3 concentration. For hierarchical clustering, selected parameters (pH, EC, T, DO and alkalinity) were used for calculating Euclidean distance matrix, and clustering was done with UPGMA (Unweighted Pair Group Method with Arithmetic Mean) method in R with vegan, ggplot2 and ggdendro packages (Oksanen et al., 2025, de Vries & Ripley, 2024, Wickham, 2016). Water for hydrogeochemical analyses including isotopes was taken into the sample bottles immediately from the end of the pumping tube and the sample pretreatment, filtering and acidification, was performed in the field after sampling. Water samples for oxygen and hydrogen isotope analyses were collected without pretreatment and stored in 60 mL high-density polyethylene (HDPE) bottles. For isotopic analyses of strontium and sulphur groundwater was filtered with a 0.45 µm Ca-S filter into acid-washed 250 ml bottles and acidified with ultrapure 13.8 N HNO_3 (5 ml per sample bottle). Treated samples were kept cool during field work and transportation to the laboratory. The chemical parameters from the water samples were analysed by the Eurofins Labtium laboratory (Espoo, Finland). Dissolved element concentrations were analysed with ICP-MS and anion concentrations (Br-, Cl-, F, NO^3- ja SO_4^{2-}) with ion chromatography. The dissolved and total organic carbon (DOC, TOC) were also analysed at the Eurofins Labtium.

2.2 Isotope hydrogeochemistry analysis

The isotopic compositions of oxygen, hydrogen, strontium and sulphur from the water samples were analysed in the GTK research laboratory in Espoo, Finland. Sample waters for the $\delta^{18}O$ and $\delta^{2}H$ analyses were filtered in the laboratory and analysed with a Picarro L2130i CRDS (Cavity Ring Down Spectroscopy) analyser. The measurement uncertainty for $\delta^{18}O$ being < 0.1 ‰, and for $\delta^{2}H$ < 0.3 ‰. For the $^{87}Sr/^{86}Sr$ analysis, a concentration-dependent amount of prefiltered and -acidified samples were evaporated to dryness and dissolved with ultrapure 3.2 N HNO_3 for ion exchange. Strontium was eluted with ultrapure 0.05N HNO_3 acid by 100 µl of Sr-specific resin (TrisKem Sr Resin, 50−100 µm). For the measurement, the samples were diluted to a Sr concentration of approx. 20 ppb (in ultrapure 2% HNO_3). The analyses were carried out by using an Aridus 3 Desolvating system (DSN) with 50µl PFA ConcentricFlow nebulizer and a Multi-Collector Inductively Coupled Plasma Mass Spectrometer (MC-ICP-MS, Nu Instruments™) at low mass resolution (Δm/m = 400). The isotopic measurements were performed in static mode using five faraday detectors, and 10 blocks of 6 integrations of approximately 8 s. The standard reference material NBS987, was used to monitor the precision and accuracy of the measurements at the beginning, and the end of every session and after every fifth sample. The obtained average of $^{87}Sr/^{86}Sr$ was 0.710270 (± 0.000066, 2 sd, n=5), which is close to the reference value 0.710250 (± 0.00004, 2 sd, n=2306, GEOREM database, http://georem.mpch-mainz.gwdg.de/). Prior to the $\delta^{34}S$ analysis, samples were eluted following the classic liquid column chromatography technique (Paris et al., 2013). Based on the sulphur concentration, part of the filtered and acidified sample was evaporated to dryness and dissolved with ultrapure 0.25 % HCl. Cations were removed with BioRad AG50X8 resin and samples were further diluted with ultrapure 2 % HNO_3 to approx. 0.25 ppm concentration. Sodium was added to the samples (0.5 ppm) before the analysis to improve the sensitivity of sulphur (Yu et al., 2017). The analyses were carried out using an Aridus 3 Desolvating system (DSN) with 50µl PFA ConcentricFlow nebulizer and a MC-ICP-MS (Nu Instruments ™) at medium mass resolution (Δm/m = 3000). The S

isotopic measurements were performed in static mode using three faraday detectors, and 3 blocks of 20 integrations of 8 s. The average value of the IAEA standard S-3 was - 32.0 (± 0.3, 1sd, n=5), while the recommended values is -32.2 (±0.4 ‰ 1sd, n=36, Georem database, http://georem.mpch-mainz.gwdg.de/).

2.3 Residence time indicator sampling and analysis

Atmospheric CFC concentrations increased since the late 1940 to early 1990 and are nearly stable in the atmosphere. During recharge these tracers are dissolved in the water and transported with the flow. The CFC concentrations in water depend not only on the time of recharge, but also on the recharge temperature of the water, additional dissolved air bubbles (so-called excess air) and degradation in un-oxic environment. SF6 has been released decades later. Atmospheric concentrations are still increasing but are still much lower than for CFCs. Due to the very low solubility excess air effects the signal even more. Also, in granite rocks SF6 is produced by natural sources on long time scales.

The radioactive hydrogen isotope tritium (^3H) with a half-live of 12.32yrs is bound to the water molecule in precipitation. Tritium concentrations in precipitation increased since the mid-1950s to about 1962 by 3 orders of magnitude compared to the natural concentrations on the northern hemisphere. Since 2010 concentrations are nearly back to natural levels (Cauquoin et al. 2024). Tritium is a suitable tracer to detect water recharged since the late 1950ies, which is called young water.

In combination with the decay product of tritium, the light helium isotope ^3He, it is possible to calculate the groundwater residence time without knowledge of the initial tritium input. The challenge is to separate ^3He from tritium decay (tritiogenic ^3He) from other He sources. Atmospheric ^3He is dissolved in surface water according to the water temperature at recharge. The water can contain additional air bubbles (excess air) and depending on the rock matrix also terrigenic ^3He. This is produced by neutrons reacting with ^6Li which produces ^3H, and hence ^3He. The neutrons came from U and Th decay and secondary reaction and are coming along with ^4He from alpha-decay of U and Th. So, in old water ^4He and ^3He can be increased. The concentrations and $^3He/^4He$ ratio depend on the rock matrix composition and the release rate from the rock to the surrounding water body. This results in significant uncertainties for the $^3He/^4He$ ratio of terrigenic He. And hence, inhibits for large He concentrations the separation of tritiogenic ^3He. Tritiogenic ^3He ($^3He_{tri}$) is calculated as follows from the components: $^3He_{tri} = {}^3He_{meas} - {}^3He_{equi} - {}^3He_{excess} - {}^3He_{terr}$; $^3He_{meas}$: measured concentration, $^3He_{equi}$: solubility equilibrium concentration, $^3He_{excess}$: excess air concentration derived from Ne, $^3He_{terr}$: terrigenic He concentration derived from ^4He. The uncertainties for each component add up to uncertainty for $^3He_{tri}$. A detailed explanation on the different ^3He contribution can be found in Kipfer et al. (2002). Samples of groundwater for CFCs and SF_6 analysis were collected in two tins, each holding a ground glass flask. The opened can and flask were placed in a bucket. Then, the pipe from the pump was placed to the bottom of the flask, which was rinsed multiple times until the bucket overflowed. After the flask was closed with a plug and secured with a clamp, the can container was closed with a circlip (underwater). CFCs and SF_6 were analysed by gas chromatography with an electron capture detector (GC-ECD) at Dr. Oster's trace substances laboratory (Wachenheim, Germany). Samples for tritium analysis were collected in 1L HDPE bottle and stored in a cold room (5°C) until analysis. Tritium was analysed at Hydroisotop GmbH

(Germany) using liquid scintillation spectroscopy LSC after electrolytical enrichment (Perkin Elmer Quantulus GCT 6220). Tritium concentrations are reported in tritium units (TU) with double standard deviation (1TU=0.119 Bq/L). Samples for noble gases analyses were collected in duplicate in clamped-off copper tubes connected to the pumping line. Noble gases (Helium isotopes and Neon) were analysed at the Bremen Mass Spectrometric Facility according to Sültenfuß et al. (2009).

2.4 Microbiological sampling and analysis

Groundwater samples were retrieved for microbial community structure analysis. As groundwater is a naturally oligotrophic environment, the microbial cell numbers were estimated to be low. Therefore, to collect enough microbial biomass for DNA amplicon sequencing analysis, 65 - 183 l of groundwater from each groundwater well was filtered by a dead-end ultrafiltration method (DEUF) with a flow rate of 2-3 l/min using a sterile silicone tubing with an ultrafiltering cartridge (ASAHI Rexeed-25A, Asahi Kasei Medical Co., Ltd., Tokyo, Japan), according to Inkinen et al. (2019). Groundwater was pumped from the wells to a 20-l plastic canister sterilized with 70% EtOH and flushed with the sampling fluid, from where the water was pumped through the DEUF capsule cartridge with a peristaltic pump. The flow-through was measured using a water meter and a 10-l bucket. DEUF-capsules were kept cool during field work and transportation to further handling the laboratory of water microbiology of the Finnish Institute for Health and Welfare, Kuopio.

Microbial biomass was eluted from the DEUF-capsules in laboratory as described in Inkinen et al. (2019). The secondary concentration of DEUF-eluates (100 - 250 mL, corresponding to sample volume of 11 - 80 L) was conducted by filtration through Millipore Express PLUS membrane filters (pore size 0.22 µm, Merck KGaA. Darmstadt, Germany) (Kauppinen et al., 2019) and stored in -75 °C before nucleic acid extraction. Total nucleic acids were extracted from the Express PLUS filters using Chemagic DNA Plant kit (Perkin-Elmer, Waltham, USA) and Kingfisher device (Thermo Fisher Scientific, Waltham, MA, USA) and DNA concentration was measured with a Qubit mini fluorometer using Qubit dsDNA HS assay (Thermo Fisher Scientific, Waltham, MA, USA) as described in Inkinen et al. (2019). Negative control samples of DEUF elution and DNA extraction were also included in the analysis. MiSeq amplicon sequencing of the 16S rRNA gene of bacteria and archaea, and ITS1 region for fungi using 2x300bp paired end protocol was done in commercial laboratory (Eurofins Genomics Ltd., Konstanz, Germany). The primers used were 341F 5'CCTACGGGNGGCWGCAG-3' (Herlemann et al., 2011) and 926R 5'-CCGYCAATTYMTTTRAGTTT-3' (Quince et al., 2011) (V3-V5) for bacteria, 340F 5'-CCCTAYGGGGYGCASCAG-3'(Gantner et al., 2011) and 806R 5'-GGACTACNVGGGTWTCTAAT-3 (Apprill et al., 2015) (V3-V4) for archaea, and 5'-GGAAGTAAAAGTCGTAACAAGG-3' and 5'-GCTGCGTTCTTCATCGATGC-3' for fungal ITS1 (White et al., 1990). Negative controls did not produce amplicons.

Sequence reads were demultiplexed and primer sequences removed before analysis applying the DADA2 (v. 1.30.0) pipeline in Rstudio using R version 4.3.2 (Callahan et al., 2016; R Core Team, 2024) for bacterial and archaeal amplicon sequence variant (ASV) detection. When inspecting the sequence reads, reverse reads of both archaea and bacteria were of poor quality, generating issues in trimming and eventually merging the reads. Thus, the analysis was continued with just forward reads.

Reads were filtered using the following parameters (TruncLen=240, maxN=0, maxEE=2, truncQ=2). This removed approximately 4% of reads in each sample. Reads were dereplicated, sequence variants inferred from unique sequences from each sample, chimeras removed, and taxonomy assigned using Silva v. 138 taxonomy database (silva_nr99_v138.1_train_set.fa) (Quast et al., 2013; Yilmaz et al., 2014) for archaea and bacteria.

Fungal sequences were analysed using the ITS-specific variation of version 1.8 of the DADA2 workflow (Callahan et al., 2016). First, ITS primer sequences were detected, primer orientation was verified, and primers were cut from the sequences using Cutadapt tool (Martin, 2011). After quality trimming with parameters: maxN = 0, maxEE = c(2, 2), truncQ = 2, minLen = 50, rm.phix = TRUE, sequence variants were inferred from unique sequences from each sample, forward and reverse reads were merged, chimeras removed and taxonomy assigned using UNITE general FASTA release (sh_general_release_dynamic_04.04.2024.fasta) (Abarenkov et al., 2024) for fungi.

DADA2-treated sequence data were imported to phyloseq (v.1.46.0) (McMurdie & Holmes, 2013) for data visualisation and statistical analyses in RStudio. Tools used in RStudio included vegan, ggplot2, dplyr, ampvis2, psadd and cowplot (Andersen et al., 2018; Oksanen et al., 2025; Wickham, 2009; Wickham et al., 2026; Wilke, 2025). Raw sequence data is deposited in NCBI's SRA under BioProject PRJNA1270735.

3 Results

3.1 Field observations and hydrogeochemistry

Field parameters and the calculated partial pressure of CO_2 (pCO_2) are presented in Table 2. The unconsolidated aquifer groundwaters had an electrical conductivity ranging from 90 to 204 µS/cm and a pH between 6.2 and 6.8, whereas the water from the bedrock borehole was more mineralized (EC 296 µS/cm) and had a higher pH (8.4). Temperature range was 5.7 -6.9 °C, and highest dissolved oxygen concentrations were measured at KUU19 and HÄJY30 (5,7 and 4,4 mg/l, respectively). The field data clustered the samples to three groups, R56 clustering clearly separate from the other sites. Oxidation-reduction potential varied significantly between the different samples from lowest in bedrock groundwater R56 (-254 mV) to highest in HÄJY11 and KUU19, corresponding to high dissolved oxygen concentrations in these samples. Highest Cl^- concentration was measured from the bedrock groundwater (R56). Alkalinity varied from 23.5 mg/l in KUU19 to 152 mg/l in R56. In all groundwater samples representative of unconsolidated aquifer waters, log partial pressure of CO_2 (pCO_2) values ranged between –1.4 and –2.2 atm while the lowest log pCO_2 value in the dataset (-3.3) was observed in bedrock groundwater.

Table 2. Field measurement data of pH, electrical conductivity (EC), temperature (T), dissolved oxygen (DO), oxygen reduction potential (ORP), alkalinity (Alk), chloride concentration (Cl-) from the sampling sites and calculated pCO2. Clustering is based on the field measurements (in bold).

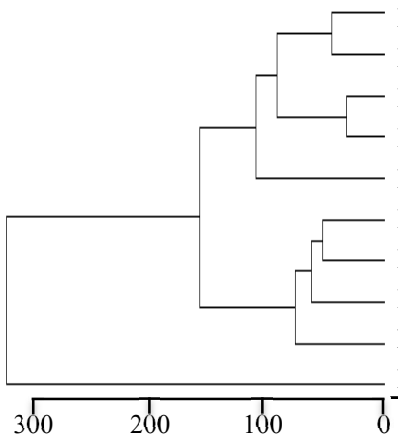

Sample ID	pH	EC	T	DO	ORP	Cl^-	Alk. (as HCO^3)	log pCO_2
		µS/cm	°C	mg/l	mV	mg/l	mg/l	atm
MIETO17	**6,3**	**124,4**	**6,4**	**3,5**	17,9	2,9	**68,3**	-1,6
MIHP6	**6,8**	**118,0**	**5,9**	**3,3**	50,5	2,2	**48,8**	-2,2
HÄJY30	**6,7**	**204,5**	**6,3**	**4,4**	-52,3	6,6	**115,9**	-1,7
KUU19	**6,4**	**89,9**	**6,2**	**5,7**	104,4	4,1	**23,5**	-2,2
LOHI30	**6,6**	**165,2**	**6,4**	**2,7**	96,0	4,6	**112,2**	-1,6
HARJA10	**6,5**	**178,8**	**5,7**	**3,4**	-91,6	7,1	**92,7**	-1,7
MIHP15	**6,6**	**162,7**	**6,8**	**3,9**	-50,9	n.a.*	**83,0**	-1,8
HÄJY11	**6,7**	**97,2**	**6,2**	**3,1**	109.2	1,3	**37,8**	-2,2
NOPPA15	**6,2**	**188,8**	**6,1**	**2,7**	-0,2	10,8	**78,1**	-1,4
R56	**8,4**	**296,2**	**6,9**	**2,7**	-254,0	26,6	**152,5**	-3,3

* n.a.: Not available, laboratory measurements of chloride concentrations are reported in Supplementary Table 1.

The major ions in groundwaters were Na (46.5mg/l in R56 to 4.82 mg/l in HARJA10), Cl (25 mg/l in R56 to 1.7 mg/l in MIHP6, see supplementary Table 1 for laboratory measurements), and Fe (31.5 mg/l in HARJA10, below the detection limit of 0.03 mg/l in HÄJY11 and KUU19 and 0.08 mg/l in MIHP6), and Ca, with highest concentrations in NOPPA15 and HÄJY30 (14.8 mg/l and 15.8 mg/l, respectively) (Supplementary Table 1). Highest sulphur and sulphate concentrations were detected from NOPPA15, and highest organic carbon concentrations were in HARJA10 groundwater (Supplementary Table 1).

Groundwater types were defined and represented on a Piper diagram (Fig. 2) showing the proportion of major ions (Na^+, Ca^{2+}, Mg^{2+}, K^+, HCO_3^-, Cl^-, SO_4^{2-}) (Piper 1944, Simler 2012). Unconsolidated aquifer groundwater samples are of calcium-bicarbonate (Ca-HCO_3) type or mixed cations-HCO_3, whereas groundwater collected from the bedrock borehole (R56) beneath the Paloluoma valley is classified as sodium-bicarbonate (Na-HCO_3) type, reflecting a more evolved groundwater. NOPPA15 has more chloride (7.6 mg/l) than the other unconsolidated aquifer samples (1.7 – 5.1 mg/l) and KUU19 has some nitrates (4.6 mg/L) (Supplementary Table 1).

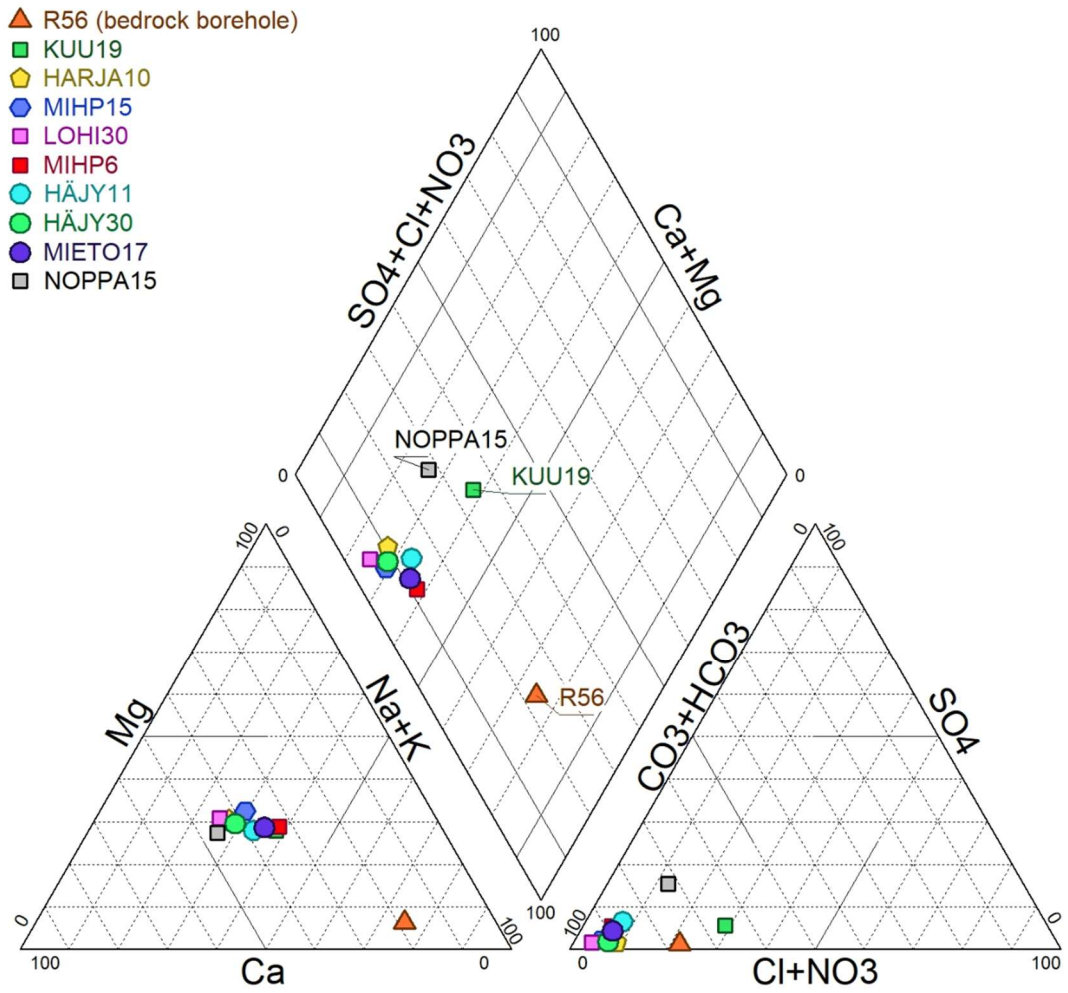

Figure 2. Piper diagram for the 10 groundwater samples collected in the study area.

305

3.2 Isotopic compositions of hydrogen and oxygen

The variation in the isotopic compositions of oxygen and hydrogen in the analysed water samples was small. The δ^2H values range from -91 to -88.2 ‰ and the $\delta^{18}O$ from -12.63 to -12.22 ‰ (with the analytical uncertainty for $\delta^{18}O$ is < 0.1 % and for δ^2H < 0.3 %). In the Fig. 3 the weighted annual average from the south-western coastal site of Olkiluoto and the eastern Finnish
310 city of Kuopio (GNIP database, IAEA), with similar latitude to the study site, are marked on the meteoric water line. The d-excess values Eq. (1), calculated from δ^2H and $\delta^{18}O$ values, ranged from 9.6 to 10.8, indicating that the sampled waters are unevaporated and of meteoric origin. This is reinforced by the fact that the samples all plot on or near the meteoric water lines (Table 3, Fig. 3).

$$d - excess = \delta^2H - 8 * \delta^{18}O \quad (1)$$

315

Table 3. The isotopic analysis results and the calculated d-excess values together with the concentrations of strontium and sulphur in the water samples.

ID	δ^2H (‰)	$\delta^{18}O$ (‰)	d-excess	$^{87}Sr/^{86}Sr$	Sr(µg/l)	$\delta^{34}S$ (‰)	S(mg/l)
NOPPA 15	-89.0	-12.42	10.4	0.74535	101	1.1	5.87
MIHP6	-91.0	-12.59	9.7	0.74029	46.7	8.0	0.7
MIHP15	-90.2	-12.63	10.8	0.72133	82.7	12.6	0.34
R56	-89.4	-12.51	10.7	0.73225	91.6	23.8	0.5
LOHI30	-89.7	-12.49	10.2	0.74159	86	30.3	0.26
KUU19	-90.8	-12.56	9.7	0.75237	38.3	5.9	0.39
HÄJY30	-89.1	-12.42	10.3	0.72832	107	14.1	0.57
MIETO17	-89.5	-12.46	10.2	0.73679	70.8	5.3	0.93
HARJA10	-89.9	-12.49	10.0	0.73713	74	18.5	<0.2
HÄJY11	-88.2	-12.22	9.6	0.73752	56.5	8.8	0.64

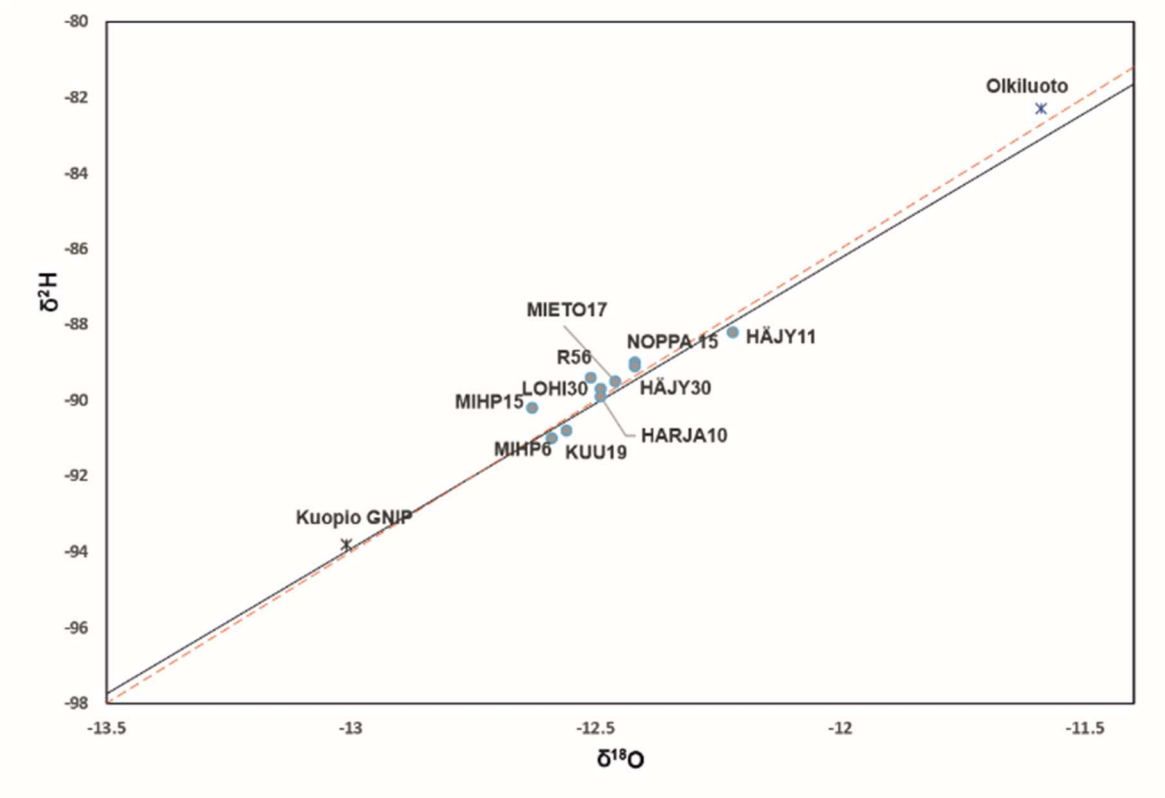

Figure 3. The isotopic compositions of oxygen and hydrogen from the water samples against the GMWL (Global Meteoric Water line) in red dashed line and the LMWL (Local Meteoric Water Line) in black. Olkiluoto weighted 8-year annual mean (https://inis.iaea.org/collection/NCLCollectionStore/_Public/46/095/46095041.pdf) and Kuopio GNIP, Global Network of Isotopes in Precipitation (https://www.iaea.org/services/networks/gnip) as references.

3.3 Isotopic compositions of Sr and S

The isotopic compositions of strontium and sulphur in the water samples vary between 0.72133 – 0.75237 and 1.1 – 30.3 ‰ respectively (Table 3). The corresponding concentrations of Sr and S in the water samples vary between 38.3 – 107 µg/l and 0.1 – 5.9 mg/l respectively (Table 3, Supplementary Table 1). Both elements show noticeable variation (Table 3).

3.4 Groundwater residence time indicators

The results of the tritium, helium isotope, neon, SF_6 and CFCs analyses are listed in Table 4. Samples NOPPA15, KUU19, HARJA10 and HÄJY11 had tritium concentrations ranging from 1.6 to 4.8 TU, while samples MIHP6, MIETO17, MIHP15, R56, LOHI30 and HÄJY30, were below the detection limit of 0.6 TU (2-sigma) (Table 4). Tritium concentrations between 1.6 and 4.8 TU (NOPPA15, KUU19, HARJA10) clearly show a modern component (0 to 60 years old). Assuming a decay-

corrected tritium concentration in precipitation to be near natural levels of 4-5 TU for Finland, then the HÄJY11 shows the presence of a modern component with significant dilution of 2/3 older tritium-free water. The absence of tritium (<0.6 TU) indicates sub-modern waters with ages exceeding 70 years. Due to the given detection limit this proportion of modern water cannot be significantly larger than 15%. Hence, only samples with tritium a calculation of ^{3}H-^{3}He ages is possible.

Table 4. Summary of measured ^{3}H concentrations, calculated tritiogenic Helium 3 ($^{3}He_{trit}$), $^{3}He/^{4}He$ ratio, calculated terrigenic Helium 4 ($^{4}He_{ter}$), CFC and SF_6 concentrations. The uncertainty of SF_6 is 20%. Tritiogenic Helium 3 was determined with an altitude of the recharge area of 150 m and a recharge temperature of 5°C.

Sample	^{3}H	$^{3}He_{trit}$	$^{3}He/^{4}He$	^{4}He	$^{4}He_{terr}$	Ne	Ne/He	SF_6	CFC11	CFC12
	TU	TU		ccSTP/g	ccSTP/g	ccSTP/g		fmol/L	pmol/L	pmol/L
NOPPA15	4.8 ± 0.6	88	3.62E-07	1.03E-06	9.31E-07	3.90E-07	0.38	18	13 ± 3	1.4 ± 0.1
MIHP6	< 0.6	-	1.61E-07	1.89E-06	1.65E-06	8.76E-07	0.46	2700	<0.05	<0.05
MIHP15	< 0.6	-	4.08E-08	7.25E-06	7.12E-06	5.06E-07	0.07	75	<0.05	<0.05
R56	< 0.6	-	2.8E-08	1.02E-04	1.02E-04	8.56E-07	0.01	27	<0.05	<0.05
LOHI30	< 0.6	-	1.30E-07	1.86E-06	1.68E-06	6.62E-07	0.36	990	0.08 ± 0.05	<0.05
KUU19	3.8 ± 0.7	107	9.40E-07	4.55E-07	3.42E-07	4.38E-07	0.96	110	230± 10	2.1 ± 0.2
HÄJY30	< 0.6	-	6.6E-08	3.70E-06	3.52E-06	6.88E-07	0.19	2200	0.5 ± 0.1	<0.05
MIETO17	< 0.6	-	7.1E-08	3.51E-06	3.34E-06	6.28E-07	0.18	100	0.19 ± 0.05	<0.05
HARJA10	4.6 ± 0.6	61	1.36E-06	1.71E-07	1.13E-07	2.49E-07	1.46	140	0.07 ± 0.05	<0.05
HÄJY11	1.6 ± 0.7	41	2.09E-07	1.98E-06	1.78E-06	7.42E-07	0.38	32	0.17 ± 0.05	0.09 ± 0.05

The applicability of CFCs and SF_6 for groundwater residence time determination is very limited for this study. The CFCs data exhibit anomalous concentrations and variable CFC11/CFC12 ratios, indicating contamination or degradation processes. The data show that tritium-free waters do not contain any CFC11 or CFC12. This means that the sampling gear is not responsible for the extreme high CFC concentrations. Concentrations of CFC113 in all samples were at or below the detection limit and were therefore excluded further analysis.

All samples showed SF_6 contents (18-2700 fmol/L) well above solubility equilibrium with modern atmosphere (approx. 4 fmol/L), indicating that the excessive groundwater concentrations derive from a local geogenic source, as frequently observed in Scandinavian groundwater systems (Åkesson et al. 2015). Consequently, CFCs and SF_6 tracers are unsuitable for groundwater age dating at this site. The data are nevertheless shown to illustrate the limitations of these methods under the studied conditions.

Seven out of ten noble gas samples have been analysed in duplicates and provided identical results. Neon concentrations reveal abnormal excess air (more than 2×10^{-7}ccSTP/g), which diminishes reliable age calculations based on noble gases. For the analysis of samples with high ^{4}He concentrations the amount of gases was split to small units. This increased the uncertainty for Ne to about 1% of the He concentration.

Samples with large excess air and non-detectable CFC concentration clearly state that the source of excess air does not result from ambient air, such as air penetration into the water during sampling. As typical groundwater recharge conditions are not expected to form this massive intrusion of excess air, the source remains unclear.

Nevertheless, He isotopes still give some insight on the age composition of the water. All samples show high ^{4}He concentrations, ranging from 4.55 $\times 10^{-7}$ to 1.0$\times$ 10^{-4} ccSTP/g, which is equivalent to 4-2200 times the solubility equilibrium, indicating a significant source of terrigenic He. The ^{3}He/^{4}He ratios in tritium-free samples range from 3×10^{-8} to 7×10^{-8}, which are significantly lower than the ratios typical of atmospheric or mantle He. The ^{3}He/^{4}He ratio of $5\times10^{-8} \pm 2\times10^{-8}$ is used for the terrigenic He component in the calculation of tritiogenic ^{3}He for samples with tritium. Excess air is assumed to be free of tritiogenic ^{3}He (Fig. 4). Both error sources result in an error from tritiogenic ^{3}He of 25%. However, even with the large uncertainties the ^{3}H-^{3}He ages of NOPPA15, KUU19, HARJA10 and HÄJY11 are between 47 and 59 years (± 25%). These results suggest groundwater residence times substantially longer than 30 years. The presence of high radiogenic Helium 4 (^{4}He$_{rad}$) indicates the presence of old groundwater (several thousand years old). The only bedrock borehole R56 has the highest radiogenic helium contents of all the wells.

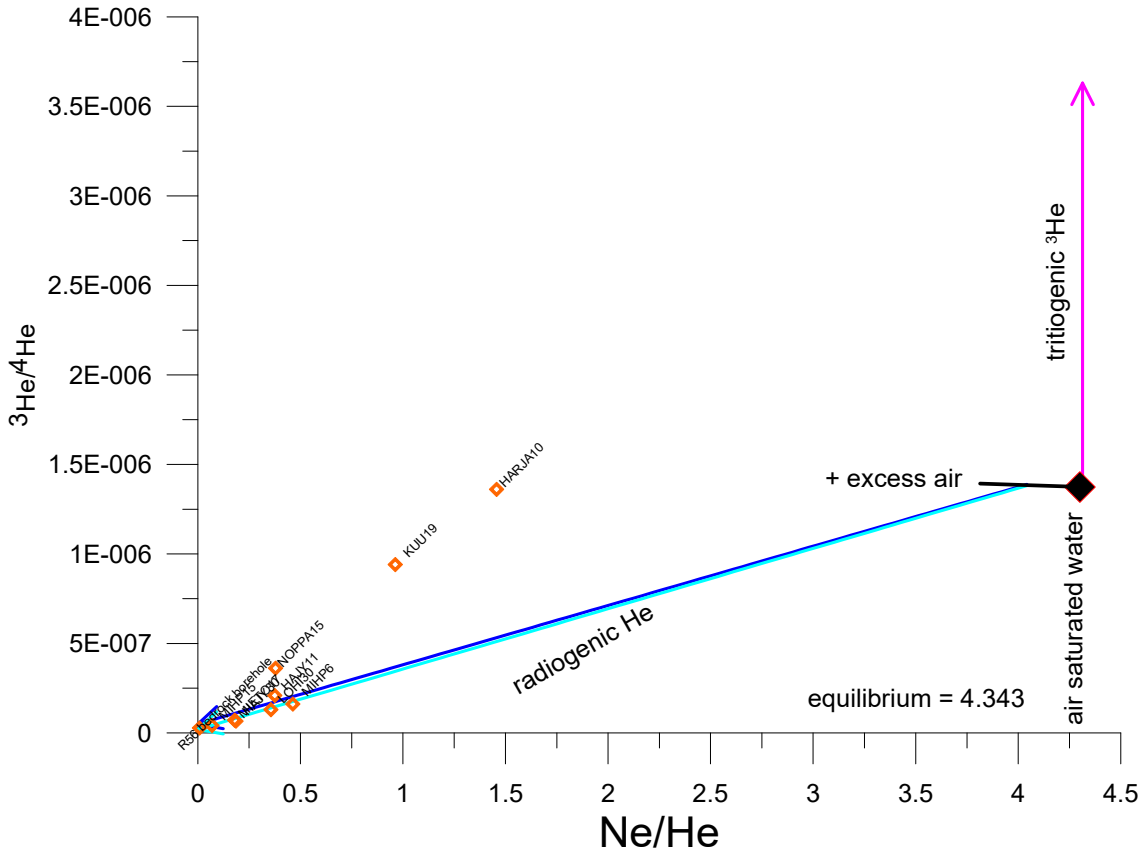

Figure 4. Ratios of He isotopes vs. Ne/He ratios of all samples. The light blue line shows mixing of water equilibrated at 5°C plus 30% of excess air with terrigenic He with a ^{3}He/^{4}He of 2×10^{-8}, the dark blue line ratio of ^{3}He/^{4}He 5×10^{-8}. The vertical offset from this line indicates tritiogenic ^{3}He.

3.5 Microbial communities

Bacterial 16S rRNA amplicon sequencing was successful from HARJA10, HÄJY30, LOHI30, MIETO17, MIHP15, NOPPA15 and R56. Altogether 996 645 bacterial sequences were retrieved of these, and after quality filtering, denoising and chimera removal steps, 90-94% of the reads were retained in each sample. Altogether 71 different bacterial phyla were detected and ASVs belonging most prevalently to Patescibacteria, Verrucomicrobiota, Chloroflexi and Proteobacteria (Supplementary Table 2., 3.). Bacterial communities were diverse and varied from borehole to borehole (Fig. 5a, Supplementary Figure 1a). NOPPA15 hosted the most diverse bacterial community according to Shannon index (H' 6.69), while MIHP15 and bedrock groundwater well R56 exhibited the lowest observed Shannon diversity (H' 3.63 and 2.91, respectively) (Fig. 5a, Supplementary Table 2.). These communities were more similar with each other compared to other sites. Relatively most abundant bacterial ASVs detected from NOPPA15 affiliated with *Gallionella* (12% relative abundance), *Omnitropha* (10%) and several candidate genera of Patescibacteria phyla. The bedrock borehole water R56 hosted a bacterial community with abundant sulfate reducers such as Desulfovibrio (38% relative abundance) in addition to *Hydrogenophaga* (11%), *Ferribacterium* (9%) and *Acetobacterium* (8%). Of these, *Hydrogenophaga* -affiliating ASVs were either absent or found in very low abundance (<0.2%) in other samples. *Desulfovibrio* and *Acetobacterium* ASVs were also most abundant in MIHP15 (57% and 11%, respectively). Sulfate reducing *Desulfosporosinus* was also most abundant in HÄJY30 (65% of the bacterial community), together with *Candidatus* Omnitrophus (12% relative abundance) and Patescibacteria -affiliating ASVs (altogether 7% of total bacterial community). MIETO17 hosted almost as diverse bacterial community as NOPPA15 according to Shannon diversity index (H' 6.52). Abundant ASVs in MIETO17 affiliated with Desulfobacterota (10%), Dehalococcoidia (9%), *Rhodoferax*, *Omnitrophus* and Patescibacteria (6% relative abundance each), Nitrospirota (4%) and Sva0485, recently named as *Candidatus* Acidulodesulfobacterales (Tan et al. 2019) (3%). Most common ASVs in LOHI30 were *Candidatus* Omnitrophus (13%), *Ferribacterium* (8%), *Acetobacterium* (8%), Dehalococcoidia (7%), *Rhodoferax* (6%), *Desulfurivibrio* (6%), and *Gallionella* (4%). Similarly, in HARJA10, *Candidatus* Omnitrophus was among the most dominant ASVs (13% relative abundance) together with Desulfobacterota (16%), Sva0485 (10%) and Dehalococcoidia (8%).

Archaeal 16S rRNA amplicon sequencing was successful from HARJA10, HÄJY30, MIETO17, MIHP15, NOPPA15 and R56. In total 902 598 archaeal sequences were retrieved, and after quality control and chimera removal steps, 93-96% of the reads were retained (Supplementary Table 2.). A total of 11 different archaeal phyla were identified, and most prevalent phyla were Nanoarchaeota, Micrarchaeota and Crenarchaeota (Supplementary Table 3.). NOPPA15 hosted the most diverse archaeal community (H' 5.97), similar to bacteria (Fig. 5b, Supplementary Table 2.). Most archaeal sequences were affiliated with Nanoarchaota phylum in NOPPA15, HÄJY30, MIETO17 and HARJA10, with ASVs belonging to *Woesearcheales* candidate order (74%, 75%, 54%, 40% relative abundances, respectively) (Fig. 5b, Supplementary Figure 1b). Bathyarchaea -affiliating archaeal ASVs were also relatively abundant in these samples. *Candidatus* Methanoperedens and *Methanomassiliicoccales* -

affiliating ASVs were abundant in HARJA 10 (18% and 7% relative abundance, respectively), and in R56 (21% and 6%). R56 also had a 11% relative abundance of *Methanobacterium*, in addition to abundant *Woesearchales* (23%) and Bathyarchaeia (20%). MIHP15 hosted the least diverse archaeal community (H' 2.05) that differed from other samples (Fig. 5b, Supplementary Table 2). *Methanoregula*, *Methanobacterium*, and *Methanospirillum* -affiliating ASVs were dominating the archaeal community in this borehole (50%, 28% and 12 % relative abundances, respectively).

Fungal ITS1 amplicon sequencing was successful from the same samples as archaea. Altogether 649 988 sequences were retrieved, but after rigorous quality filtering and chimera removal steps, on average only 41% of sequences were kept (Supplementary Table 2.). This level was somewhat expected because of high natural length variability of fungal ITS amplicons and typically lower quality of reverse reads that are dropped from the analysis together with their forward pair. Filtering primarily removed low-quality reads and improved the accuracy of ASV inference. According to the Shannon index, the most diverse fungal community was observed in R56 (H' 4.04) and least diverse in MIHP15 (H' 2.22) (Fig. 5c, Supplementary Table 2.). Most of the detected fungal phyla belonged to either Ascomycota or Basidiomycota, and relatively most abundant ASVs affiliated with Cladosporium and *Bulleribasidiaceae* (Fig. 5c, Supplementary Figure 1c). In addition to these, R56 fungal community was composed of *Claviceps* and *Rhodotorula* (8% and 6% relative abundances). Fungal communities in NOPPA15, HÄJY30, MIHP15 and MIETO17 all had *Filobasidium* -affiliating ASVs (7%, 9%, 5% and 13% of the community, respectively). *Itersonilia* affiliating ASV was more typical to HÄJY30 (9%) than to other samples, and *Melanommataceae* -affiliating ASV was most relatively most abundant in NOPPA15 (7%). A large portion (57%) of the fungal community in HARJA10 could not be identified beyond kingdom-level.

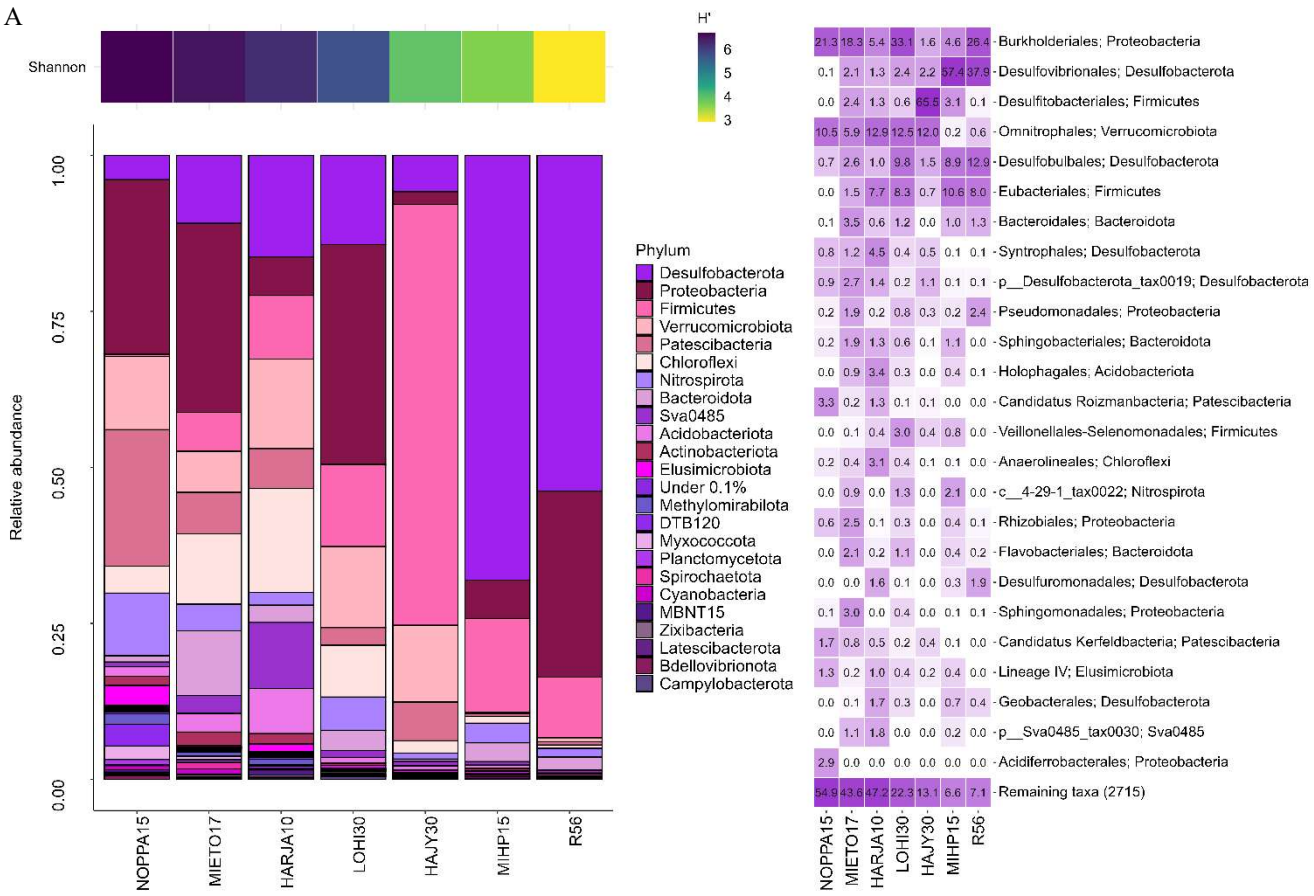
A
Shannon
H'
6
5
4
3
Relative abundance
0.00
0.25
0.50
0.75
1.00
NOPPA15
MIETO17
HARJA10
LOHI30
HAJY30
MIHP15
R56
Phylum
Desulfobacterota
Proteobacteria
Firmicutes
Verrucomicrobiota
Patescibacteria
Chloroflexi
Nitrospirota
Bacteroidota
Sva0485
Acidobacteriota
Actinobacteriota
Elusimicrobiota
Under 0.1%
Methylomirabilota
DTB120
Myxococcota
Planctomycetota
Spirochaetota
Cyanobacteria
MBNT15
Zixibacteria
Latescibacterota
Bdellovibrionota
Campylobacterota
21.3 18.3 5.4 33.1 1.6 4.6 26.4 Burkholderiales; Proteobacteria
0.1 2.1 1.3 2.4 2.2 57.4 37.9 Desulfovibrionales; Desulfobacterota
0.0 2.4 1.3 0.6 85.5 3.1 0.1 Desulfitobacteriales; Firmicutes
10.5 5.9 12.9 12.5 12.0 0.2 0.6 Omnitrophales; Verrucomicrobiota
0.7 2.6 1.0 9.8 1.5 8.9 12.9 Desulfobulbales; Desulfobacterota
0.0 1.5 7.7 8.3 0.7 10.6 8.0 Eubacteriales; Firmicutes
0.1 3.5 0.6 1.2 0.0 1.0 1.3 Bacteroidales; Bacteroidota
0.8 1.2 4.5 0.4 0.5 0.1 0.1 Syntrophales; Desulfobacterota
0.9 2.7 1.4 0.2 1.1 0.1 0.1 p__Desulfobacterota_tax0019; Desulfobacterota
0.2 1.9 0.2 0.8 0.3 0.2 2.4 Pseudomonadales; Proteobacteria
0.2 1.9 1.3 0.6 0.1 1.1 0.0 Sphingobacteriales; Bacteroidota
0.0 0.9 3.4 0.3 0.0 0.4 0.1 Holophagales; Acidobacteriota
3.3 0.2 1.3 0.1 0.1 0.0 0.0 Candidatus Roizmanbacteria; Patescibacteria
0.0 0.1 0.4 3.0 0.4 0.8 0.0 Veillonellales-Selenomonadales; Firmicutes
0.2 0.4 3.1 0.4 0.1 0.1 0.0 Anaerolineales; Chloroflexi
0.0 0.9 0.0 1.3 0.0 2.1 0.0 c__4-29-1_tax0022; Nitrospirota
0.6 2.5 0.1 0.3 0.0 0.4 0.1 Rhizobiales; Proteobacteria
0.0 2.1 0.2 1.1 0.0 0.4 0.2 Flavobacteriales; Bacteroidota
0.0 0.0 1.6 0.1 0.0 0.3 1.9 Desulfuromonadales; Desulfobacterota
0.1 3.0 0.0 0.4 0.0 0.1 0.1 Sphingomonadales; Proteobacteria
1.7 0.8 0.5 0.2 0.4 0.1 0.0 Candidatus Kerfeldbacteria; Patescibacteria
1.3 0.2 1.0 0.4 0.2 0.4 0.0 Lineage IV; Elusimicrobiota
0.0 0.1 1.7 0.3 0.0 0.7 0.4 Geobacterales; Desulfobacterota
0.0 1.1 1.8 0.0 0.0 0.2 0.0 p__Sva0485_tax0030; Sva0485
2.9 0.0 0.0 0.0 0.0 0.0 0.0 Acidiferrobacterales; Proteobacteria
54.9 43.6 47.2 22.3 13.1 6.6 7.1 Remaining taxa (2715)
NOPPA15
MIETO17
HARJA10
LOHI30
HAJY30
MIHP15
R56

425

B

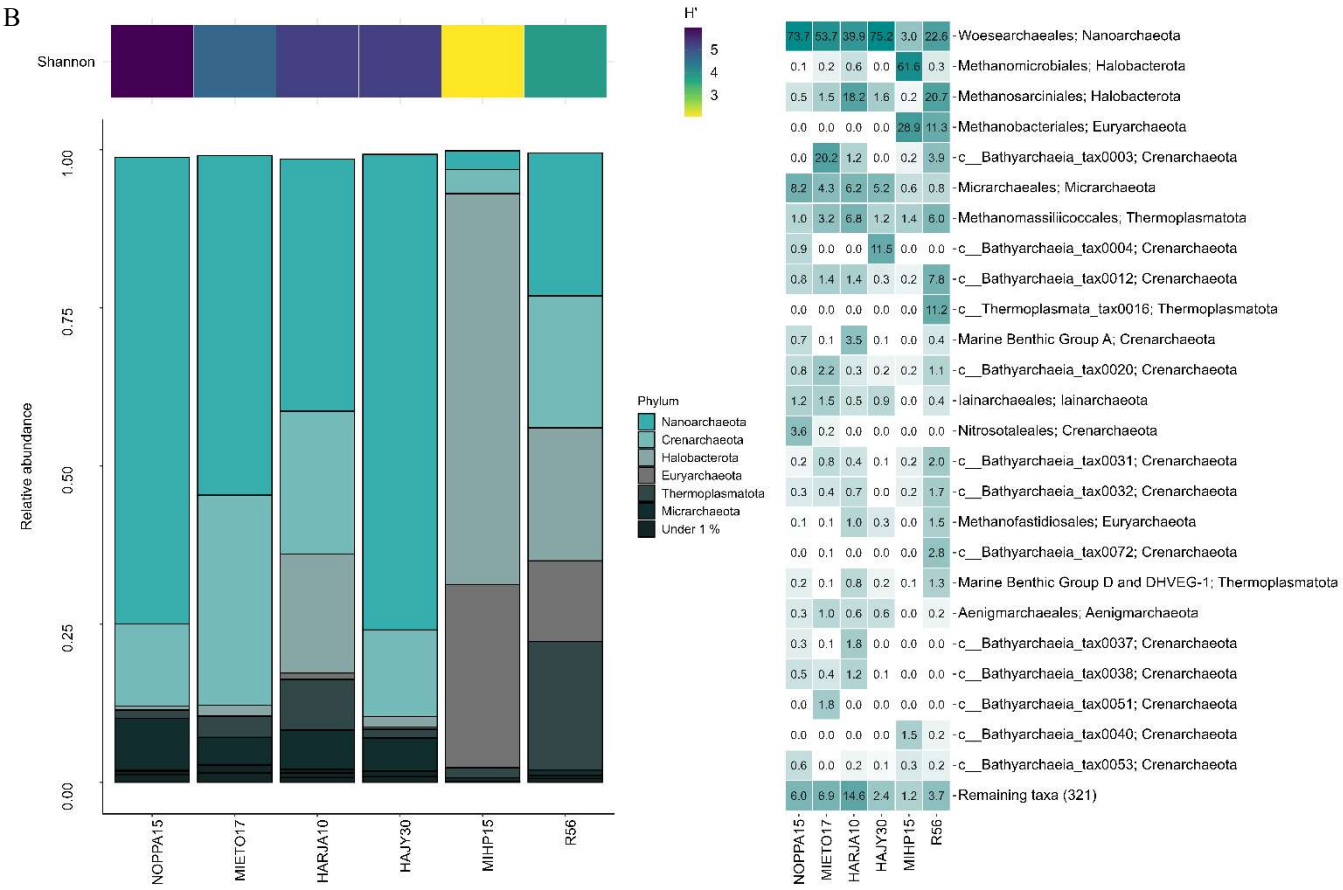
Shannon
H'
5
4
3
Relative abundance
0.00
0.25
0.50
0.75
1.00
NOPPA15
MIETO17
HARJA10
HAJY30
MIHP15
R56
Phylum
Nanoarchaeota
Crenarchaeota
Halobacterota
Euryarchaeota
Thermoplasmatota
Micrarchaeota
Under 1 %
73.7 53.7 39.9 75.2 3.0 22.6 -Woesearchaeales; Nanoarchaeota
0.1 0.2 0.6 0.0 61.6 0.3 -Methanomicrobiales; Halobacterota
0.5 1.5 18.2 1.6 0.2 20.7 -Methanosarciniales; Halobacterota
0.0 0.0 0.0 0.0 28.9 11.3 -Methanobacteriales; Euryarchaeota
0.0 20.2 1.2 0.0 0.2 3.9 -c__Bathyarchaeia_tax0003; Crenarchaeota
8.2 4.3 6.2 5.2 0.6 0.8 -Micrarchaeales; Micrarchaeota
1.0 3.2 6.8 1.2 1.4 6.0 -Methanomassiliicoccales; Thermoplasmatota
0.9 0.0 0.0 11.5 0.0 0.0 -c__Bathyarchaeia_tax0004; Crenarchaeota
0.8 1.4 1.4 0.3 0.2 7.8 -c__Bathyarchaeia_tax0012; Crenarchaeota
0.0 0.0 0.0 0.0 0.0 11.2 -c__Thermoplasmata_tax0016; Thermoplasmatota
0.7 0.1 3.5 0.1 0.0 0.4 -Marine Benthic Group A; Crenarchaeota
0.8 2.2 0.3 0.2 0.2 1.1 -c__Bathyarchaeia_tax0020; Crenarchaeota
1.2 1.5 0.5 0.9 0.0 0.4 -Iainarchaeales; Iainarchaeota
3.6 0.2 0.0 0.0 0.0 0.0 -Nitrosotaleales; Crenarchaeota
0.2 0.8 0.4 0.1 0.2 2.0 -c__Bathyarchaeia_tax0031; Crenarchaeota
0.3 0.4 0.7 0.0 0.2 1.7 -c__Bathyarchaeia_tax0032; Crenarchaeota
0.1 0.1 1.0 0.3 0.0 1.5 -Methanofastidiosales; Euryarchaeota
0.0 0.1 0.0 0.0 0.0 2.8 -c__Bathyarchaeia_tax0072; Crenarchaeota
0.2 0.1 0.8 0.2 0.1 1.3 -Marine Benthic Group D and DHVEG-1; Thermoplasmatota
0.3 1.0 0.6 0.6 0.0 0.2 -Aenigmarchaeales; Aenigmarchaeota
0.3 0.1 1.8 0.0 0.0 0.0 -c__Bathyarchaeia_tax0037; Crenarchaeota
0.5 0.4 1.2 0.1 0.0 0.0 -c__Bathyarchaeia_tax0038; Crenarchaeota
0.0 1.8 0.0 0.0 0.0 0.0 -c__Bathyarchaeia_tax0051; Crenarchaeota
0.0 0.0 0.0 0.0 1.5 0.2 -c__Bathyarchaeia_tax0040; Crenarchaeota
0.6 0.0 0.2 0.1 0.3 0.2 -c__Bathyarchaeia_tax0053; Crenarchaeota
6.0 6.9 14.6 2.4 1.2 3.7 -Remaining taxa (321)
NOPPA15
MIETO17
HARJA10
HAJY30
MIHP15
R56

C

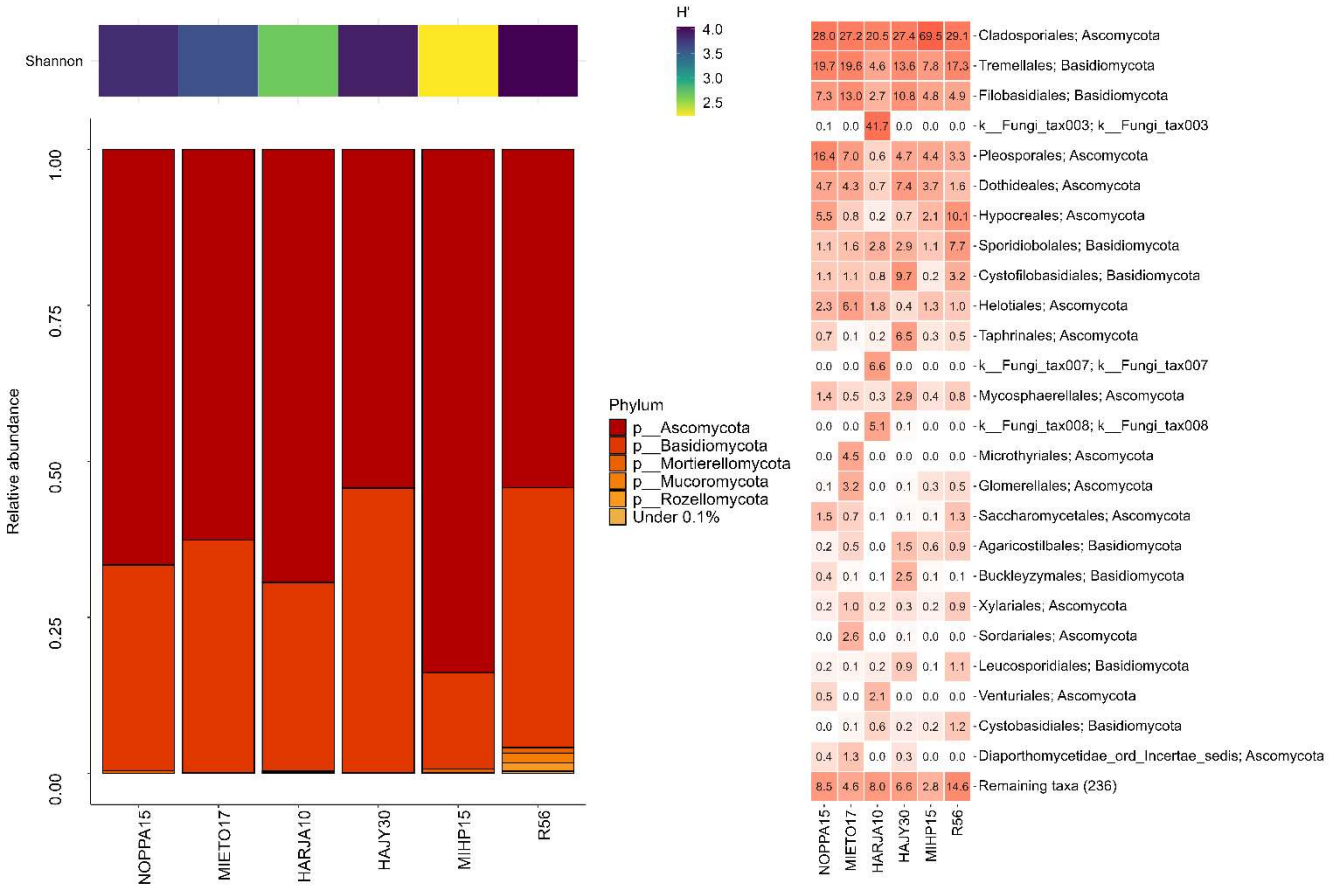

Figure 5. Groundwater microbial communities. Bar plots show the relative abundances of different A) bacterial, B) archaeal, and C) fungal phyla and heatmaps represent 25 most abundant orders of A) bacteria, B) archaea and C) fungi.

4 Discussion

Hydrogeological studies rely on use of various tracers, most often field measurement data and laboratory analysis of chemical parameters, i.e., main ion and trace element concentrations. Natural tracers have been expanded to include the use of different isotopes and microbial communities in addition to groundwater age revealing gases (CFCs, SF_6). These techniques can be used to assess the physical, biological and chemical processes that take place in a hydrogeological setting (Divine and McDonnell 2005).

4.1 The origin and age of groundwater in Kurikka according to tested tracers

Geochemistry of the sampled water provided initial information about the origin of groundwater in the complex aquifer system in Kurikka. The distinct EC values between unconsolidated aquifer groundwaters (90-204 µS/cm) and bedrock groundwater (296 µS/cm) indicate different mineralization levels. Higher EC in bedrock groundwater suggests more evolved water, indicating longer residence time allowing for mineral weathering influencing total dissolved solids (TDS). Similarly, pH differences (6.2-6.8 in unconsolidated aquifer groundwater vs. 8.4 in bedrock groundwater) suggest longer interaction time with minerals. In deep bedrock environment in Finland, where fluids have retention times of tens of millions of years, groundwaters also have high TDS, EC and pH (Kietäväinen et al. 2013). Major ion composition provided similar characterization of groundwater types. Unconsolidated aquifer groundwater being calcium-bicarbonate (Ca-HCO_3) or mixed cations-HCO_3 type, and bedrock groundwater being sodium-bicarbonate (Na-HCO_3) type, indicate different geochemical processes and sources. Often the presence of nitrates and higher chloride levels can indicate anthropogenic influences, such as agriculture, or recent recharge events in groundwater. However, noticeably higher Cl^- concentrations from bedrock groundwater are more likely to originate from the long water-rock interaction rather than anthropogenic influence. The partial pressure of CO_2 (pCO_2) provides insight into the extent to which groundwater interacts with CO_2 produced in the soil (Clark 2015). As water infiltrates the subsurface, it first passes through the unsaturated soil zone, where it equilibrates with carbon dioxide produced by the decomposition of organic matter and root respiration. This results in pCO_2 levels that are higher than those in the atmosphere (Freeze and Cherry, 1979; Appelo and Postma, 2004). Groundwater with a log pCO_2 over –2.0 indicates an open CO_2 system (Clark 2015). In all water samples representative of unconsolidated aquifer groundwaters, pCO_2 values higher than the atmospheric values suggest open-system conditions where groundwater is in equilibrium with the "soil zone" CO_2. In contrast, the pCO_2 value in bedrock groundwater suggests closed-system conditions, without CO_2 input from the soil zone.

The δ^2H and $\delta^{18}O$ values from the sampled waters lie on or near the meteoric water lines except for the R56 and MIHP15 samples, that plot, albeit very slightly, above the meteoric water lines. Bedrock groundwater samples plot normally above the meteoric water line in case they have experienced long-term water-rock interaction (Kietäväinen et al. 2013). The longer residence time enables the abiotic chemical processes in the water-rock interaction, that can fractionate the isotopic compositions of the water stable isotopes (Kietäväinen et al. 2013). These processes may also explain the MIHP15 water sample plotting slightly above the meteoric water lines, since the MIHP15 well reaches the lowermost aquifer, and most likely has active hydraulic connections to the fractured bedrock below.

The local geology is rich in silicate minerals (biotite paragneiss, granite and diorite) that have a relatively high rubidium content. Rubidium ^{87}Rb decays to ^{87}Sr, and the enriched $^{87}Sr/^{86}Sr$ values could imply either felsic mineralogy in the study area or the process of silicate weathering, both of which produce heavier strontium isotopic compositions (Ikonen et al. 2025, Négrel et al. 2018). The isotopic composition of strontium in the groundwater samples from the study site varied significantly. Although the bedrock in Kurikka is rich in rubidium-bearing mica (biotite, muscovite) minerals, which produce enriched Sr isotopic values to the bedrock groundwater, the Sr isotopic composition in the R56 bedrock groundwater sample was lower than in most of the unconsolidated aquifer water samples, excluding HÄJY30 and MIHP15. This would suggest mixing with

groundwater that is enriched in ^{87}Sr from a different mineralogical locality or heterogeneity in the geochemistry of the aquifer system. A study done in Palmottu, southern Finland, with a similar geology to Kurikka, found the $^{87}Sr/^{86}Sr$ values ranging between 0.71999 and 0.75079 in the bedrock groundwater samples (Négrel et al. 2003), which correspond to R56, but also to the rest of the samples here. If there are hydraulic connections, the mixing of different $^{87}Sr/^{86}Sr$ end-member waters is the most likely explanation for the varying Sr isotopic compositions also in the lower-most unconsolidated aquifer water samples.

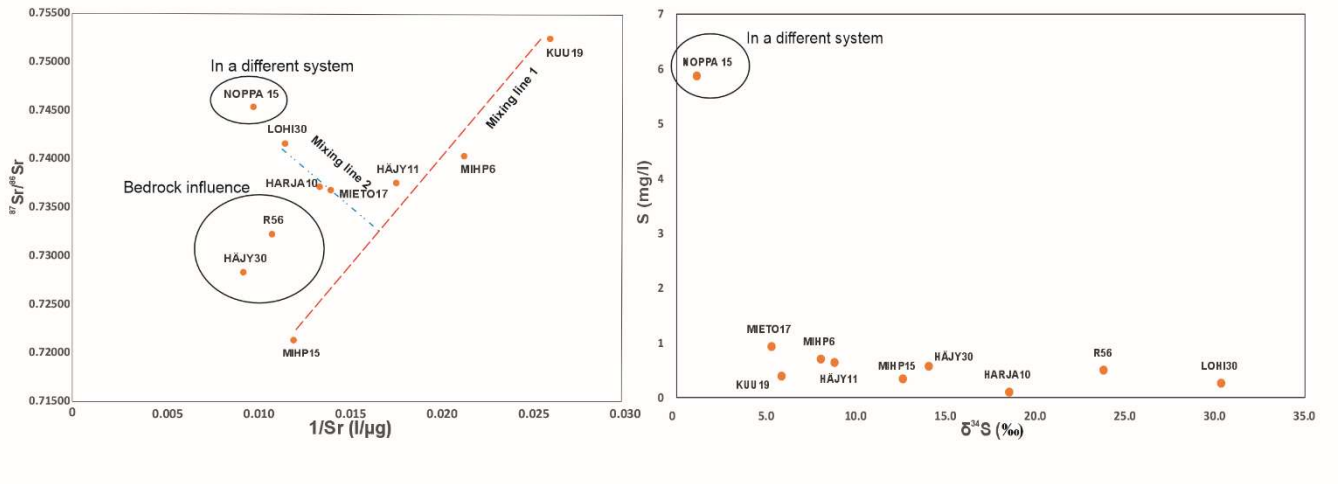

Figure 6. On the left $^{87}Sr/^{86}Sr$ values vs. the reciprocal of the Sr concentration with mixing lines (red and blue dotted lines) suggesting several endmembers. NOPPA15 is marked as belonging to a different geochemical environment due to the geology of the area and the characteristics of the groundwater well. Bedrock influence connects the two outliers R56 and HÄJY30. On the right the sulphur concentration vs. the isotopic composition of sulphur ($\delta^{34}S$) in permille. NOPPA15 marked again as representing a different system.

In a diagram with the reciprocal of the Sr concentration a binary mixing line draws as a straight line. Here the two dotted lines (red and blue) represent binary mixing trends. The samples near the red dotted mixing line (MIHP15, HÄJY11, MIHP6 and KUU19), represent influence of the Paloluoma and Häjyluoma buried valley modern/young groundwater. The sample points MIHP15 and MIHP6 are located fairly near the Kyrönjoki valley, but the natural flow of groundwater in the Paloluoma valley towards south has a volume that overrides the influence of the larger Kyrönjoki valley groundwater in those sites (Fig .1). The remaining samples on the blue mixing line (LOHI30, HARJA10 and MIETO17) represent the Kyrönjoki valley groundwater, central part of the buried valley aquifer system where there is northbound groundwater flow (Fig. 1). The mixing line does not clearly represent this south-north direction, due to hydraulic connections from the large watershed that exists west of LOHI30 (Åberg et al. 2026: Appendix A1; Fig. 3). The sample point NOPPA15 is located north of the buried valley site, and the water sample represents a different geological and geochemical environment representing topmost part of the shallow sedimentary sequence outside the buried valley aquifer system. Therefore, it is most unlikely that there is a hydraulic connection between NOPPA15 and the other sampling sites although it appears as a continuation of the blue mixing line (Fig. 6). R56 and HÄJY30

show non-conservative behaviour outside the two mixing lines that suggest three endmembers. This is most likely explained by bedrock groundwater influence. While R56 is a bedrock groundwater well, HÄJY30 is situated in the most central part of the aquifer system on the bedrock fracture zone, where highly artesian groundwater with heavy outflow character may reflect bedrock groundwater influence creating an additional endmember to the three portrayed in the diagram.

As with the isotopic compositions of strontium the variation in the $\delta^{34}S$ values is noticeable (1.1 – 30.3 ‰). Microbial processes are the most important cause of fractionation for the sulphur isotopes. Due to the microbial reduction of sulphate, the lighter ^{32}S isotope is removed from the solution (Kaplan and Rittenberg 1964). A noticeable fractionation of sulphur isotopes can be seen in the samples MIHP15, HÄJY30, HARJA10, R56 and LOHI30 with enriched $\delta^{34}S$ values ($\delta^{34}S$ >12.6). The rest of the samples KUU19, MIETO17, MIHP6 and HÄJY11, ($\delta^{34}S$ values 5.3 – 8.8 ‰), seem to reflect the atmospheric isotopic compositions of sulphur (-5 – 10 ‰) (Clark and Fritz 1997). In addition, the $\delta^{34}S$ value of NOPPA15 stands out, similarly to $^{87}Sr/^{86}Sr$, in the case of $\delta^{34}S$ with a lower isotopic composition and higher sulphur and sulphate concentration to the rest of the samples (Fig. 6). This indicates a sulphur/sulphate source with minimal heavy isotope enrichment and agrees with the microbial community structure with low abundance of sulphate reducers (see section 4.2.1 below). The oxidation-reduction potential in NOPPA15 was close to 0, so neither oxidation nor reduction reactions are strongly favoured. NOPPA15 had lighter isotopic composition of sulphur compared to other samples, suggesting minimal influence from biological processes that typically fractionate sulphur. Furthermore, different mineralogy and water flow paths from the recharge site also probably play a part in the isotope geochemistry in the sampled water from NOPPA15. Thus, NOPPA15 stands out due to its location reflecting a context of a modern esker in the Nenättömänluoma valley (Fig. 1).

Residence time tracers show the presence of a modern water component in four unconsolidated aquifer groundwater locations. This is consistent with a less evolved water type and pCO_2 values indicative of open-system conditions. In contrast, the only bedrock borehole R56 represents sub-modern water (probably some 10 000 years old, free of CFCs and ^{3}H, with the highest $^{4}He_{rad}$ concentration), with a more evolved water type, and pCO_2 values reflecting a closed system. The elevated $^{4}He_{rad}$ concentrations in all samples complicates or prevents the evaluation of groundwater residence times and mixing proportions using the ^{3}H-^{3}He technique (Shapiro et al. 1998). When radiogenic helium 4 is abundant, accurately separating the tritiogenic helium component becomes challenging and highly uncertain. The use of CFCs as tracers is constrained by their absence, localized contamination (e.g., NOPPA15, KUU19), or microbial degradation by sulphate-reducing microbes in the anoxic conditions of this environment (e.g., HARJA10) (Sonier et al. 1994).

All samples showed SF6 concentrations well above solubility equilibrium with modern atmosphere. We concluded that the excessive concentrations are derived from a local natural geogenic source (presence of granite, granodiorite). Similarly, occurrences of extreme SF_6 values due to natural sources have also been reported in southern Sweden (Åkesson et al. 2015).

Microbial diversity followed roughly the groundwater residence times. Most diverse bacterial and archaeal communities were detected from sites with a high fraction of young groundwater, while least diverse prokaryotic communities were in bedrock groundwater with old groundwater. Previous study has shown a similar distinction between old and younger groundwater microbial communities (Ben Maamar et al. 2015). This can be a result of nutrient limitation: older groundwaters are considered

more oligotrophic and energy-limited than younger groundwaters, i.e., older fluids provide a less diverse array of nutrient and energy sources for microbial inhabitants (Griebler & Lueders, 2009). Consequently, only those microbes capable of utilizing the available resources can flourish in such environments. Of the deep aquifer samples, those falling in Häjynluoma (HÄJY30) or Paloluoma (R56, MIHP15) buried valleys, were less diverse compared to those that were in between these (MIETO17, HARJA10, LOHI30). Although all sampled groundwaters were significantly younger, the diversity indices were approximately at similar level with studies of significantly deeper and older groundwater samples from Fennoscandian bedrock (Kietäväinen et al., 2014; Purkamo et al., 2016). The bedrock groundwater well R56 also hosted a microbial community with a distinct member, *Hydrogenophaga* -affiliating bacteria, which have been detected previously from older groundwaters from Canada (Ruff et al., 2023) and millions of years old, deep drillhole fluids from Fennoscandian bedrock in Finland (e.g., Purkamo et al., 2013, Kietäväinen et al., 2014).

On the other hand, fungal communities were most diverse in the bedrock well (R56) containing old groundwater, while the lowest diversity was observed in the deep unconsolidated aquifer site (MIHP15), also with a significant portion of old groundwater. This suggests that, unlike prokaryotic communities, the diversity of fungal communities is not influenced by the groundwater residence time.

4.2 Hydrogeochemistry is reflected in the microbial community structure of the groundwater

4.2.1 Sulphur

Concentrations of sulphur in the water samples were small, except for the upper aquifer water from the observation well NOPPA15 (5.87 mg/l, Fig. 6), but the values for $\delta^{34}S$ showed notable variation from 1.1 for NOPPA15 to 30.3 for LOHI30. The analysis method used for analysing the isotopic composition of sulphur from the water samples converts all the sulphur components into sulphate as described in Paris et al. (2013), and sulphide was not analysed separately. With the prevailing conditions of low organic matter, dissolved oxygen levels 2.7 mg/l or above, and at least in places high ORP, sulphur in groundwater most likely occurs mainly as sulphate. This supposition is backed by the fact that during field work no sampling site was reported as having the smell of sulphide. R56, HÄJY30, and MIHP15 samples hosted significant proportions of sulphate-reducers (e.g., *Desulfovibrio*, *Desulfosporosinus*, *Desulfurivibrio*) explaining the enrichment of the $\delta^{34}S$ values (Fig. 7). Controversially, although the LOHI30 hosts most enriched sulphur isotope composition, sulphate reducers are not abundant at LOHI30. The potential reason for this could be similar mixing as described in the Sr isotope interpretation. The lowest abundance of sulphate reducing bacteria was seen in the water sample from NOPPA15, explaining the low $\delta^{34}S$ values (Fig. 6, Fig. 7). Although sulphate is available at NOPPA15, the growth of sulphate-reducing microbes is hindered by the oxic environment. The microbial investigation demonstrated abundant sulphate-reducing bacteria affiliated with *Desulfovibrio* in R56 and MIHP15, and *Desulfosporosinus*-affiliating sulphate reducers in HÄJY30. HARJA10 had several ASVs belonging to Desulfobacterota phylum, and notable relative abundance of Sva0485, recently identified as *Candidatus*

Acidulodesulfobacterales, with potential ability to both reduction and oxidation of sulphur species, depending on the environment's oxygen availability (Tan et al., 2019).

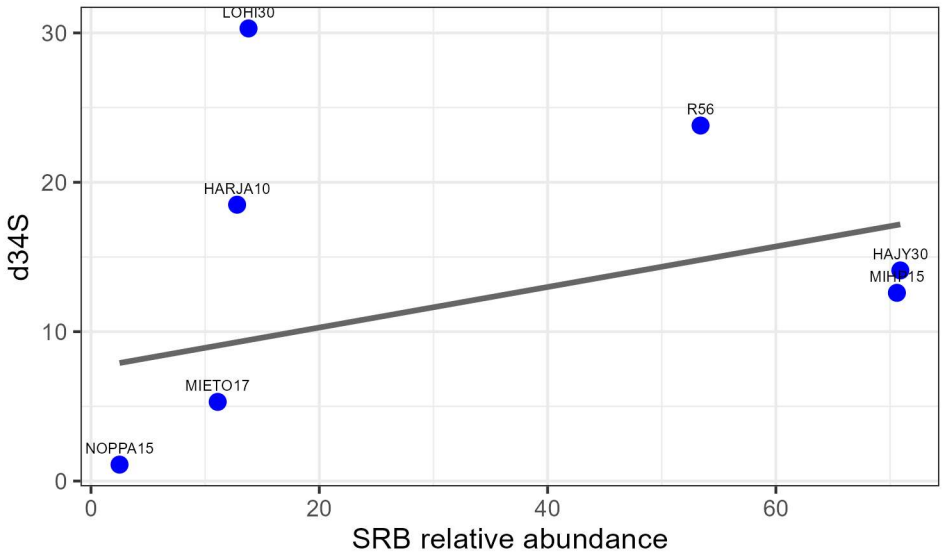

Figure 7. The relation of relative abundance of commonly identified sulphate reducers (Desulfobacterota and Desulfitobacterales among the 25 most abundant orders, see Fig. 5A) plotted against $\delta^{34}S$. LOHI30 excluded from the regression analysis.

4.2.2. Iron

Microbes associated with iron cycling were detected in most of the samples. Both MIETO17 and LOHI30 are weakly oxidising yet hypoxic and hosted known iron reducers such as a strict anaerobe *Ferribacterium* and *Rhodoferax*. *Rhodoferax* has been shown to be capable of both Fe(II) oxidation and Fe(III) reduction depending on the environmental conditions (Kato & Ohkuma, 2021). This kind of bifunctional capacity can provide an advantage for the organism in environments changing from aerobic to anoxic conditions, and lead into a significant role in iron recycling. Fe(II) oxidizers such as *Gallionella* were detected in abundance in NOPPA15, LOHI30 and MIETO17, despite the hypoxic environment. A recent pangenomic study reflected that while traditionally Gallionellaceae have been considered obligate aerobes, some may use other strategies for energy production (Hoover et al., 2023) that can explain the detection of iron oxidizers in these groundwaters. Only few iron cycling microbial taxa were detected in HARJA10 despite its highest total iron concentrations. This suggests that for example chemolithoautotrophic *Gallionellaceae*-affiliating ASVs, which were abundant at other sites, were outcompeted by other organisms. *Gallionella*-type of bacteria use inorganic carbon for growth, and iron oxidation typically occurs in environments scarce in digestible organic carbon (Hallbeck & Pedersen, 2014). In contrast, HARJA10 had abundant organic carbon, which likely supported a highly diverse and therefore more competitive microbial community.

4.2.3 Carbon

A large proportion of microbial communities in Kurikka groundwater were affiliated with heterotrophic fermenters, such as Candidatus *Omnitrophus*. Previously known as candidate phylum OP3, and currently named Omnitrophota, they are a diverse group of microbes divided to seven order-level clades. They are commonly detected in groundwater environments and have been shown to represent significant proportions of the microbial community (Perez-Molphe-Montoya et al., 2022; Suominen et al., 2021; Williams et al., 2021). *Omnitrophales* -affiliating bacteria have also been described as a type species from deep underground mine groundwaters (Momper et al., 2017). In addition to their role in mediating carbon cycling, mostly relying on organic carbon fermentation, some Omnitrophota are capable of mixotrophy and utilization of the Wood-Ljungdahl pathway to fix carbon dioxide and producing acetate (Perez-Molphe-Montoya et al., 2022). Interestingly, previous studies show dominant *Omnitrophales* or *Verrucomicrobiota* in environments with enriched elevated concentrations of trace metals, such as chromium or strontium (Bärenstrauch et al., 2022; Zhang et al., 2021). A high relative abundance of *Omnitrophus* was observed in our samples, in which Sr concentrations were highest and chromium concentrations above the detection limit.

Another potential acetate-producing microbial group, Acetobacterium, was present in some of the studied sites (HARJA10, LOHI30, MIHP15, R56). Homoacetogenic bacteria like Acetobacterium reduce CO_2 to produce acetate, using hydrogen as electron donor, therefore functioning as primary producers in groundwater (Lever, 2012). Acetate production can support not only heterotrophic microbes but also sulphate reducers by providing a continuous source of suitable substrate for energy and growth.

Similarly to previous studies, Patescibacteria-affiliating ASVs were prevalent in groundwater prokaryotic communities (Lyons et al., 2021; Schwab et al., 2017). Patescibacteria are known for their small cell size, symbiotic lifestyles and streamlined genomes. Their carbon metabolism is likely fermentative, thus Patescibacteria are contributing to breakdown and cycling of organic carbon in groundwater (Luef et al., 2015). The minimal gene array for biosynthetic and metabolic pathways makes them highly dependent on other microbes in the community, but on the other hand, they require minimal resources and are able to efficiently utilize the limited nutrients and energy sources in groundwater (Bärenstrauch et al., 2022; Chaudhari et al., 2021). Patescibacteria are abundant in both oxic and anoxic groundwaters, often co-occurring with Omnitrophota and Nitrospirota, both detected in the Kurikka aquifer system. This indicates networking and potential dependencies between these microbial components of the community (Chaudhari et al., 2021).

Archaeal communities were dominated by Woesearchaeales. These have been previously detected from groundwater environments and are believed to thrive in anoxic conditions performing fermentation-based metabolism (Castelle et al. 2015, Liu et al. 2018). Similarly, other dominant group Bathyarchaeia, have been associated with complex organic matter degradation and fermentative lifestyle (Hou et al. 2025). In R56 and HARJA10, a significant fraction of the archaeal community affiliated with freshwater anaerobic methane oxidizing archaea Methanoperedenaceae (Haroon et al. 2013), while in MIHP15, archaeal community was clearly dominated by hydrogenotrophic methanogens (Methanoregula, Methanobacterium). The reducing conditions in these samples likely create ecological niches that support the persistence of anaerobic archaea.

Despite the limited understanding of fungal metabolic capabilities in groundwater systems (Retter et al. 2024), most taxa identified here belong to saprotrophic lineages that are typically adapted to oligotrophic conditions. It is likely that the fungal communities in Kurikka sites are originating from surface environments, as many taxa are associated with soil, plant litter or phyllosphere inputs (Retter et al. 2024) and are distinct from the deeper bedrock groundwater communities such as those described in Sohlberg et al. (2015) and Purkamo et al. (2018).

4.2.4 Nitrogen

HARJA10, MIETO17 and NOPPA15 communities had abundant populations of Nitrospirae microbes in groundwater. Cultivated members of Nitrospira are known to be able to perform nitrite oxidation, complete ammonia oxidation in aerobic conditions, or anaerobic iron oxidation (Daims et al., 2015; Rosenberg et al., 2014). Recent studies highlight the importance of Nitrospirae in groundwater ecosystems and their diverse metabolic abilities (Mosley et al., 2024; Poghosyan et al., 2019; Schwab et al., 2017). Nitrospirota lineages differentiate according to oxygen availability (Mosley et al., 2024). In oxic aquifers, Nitrospirota communities differ from those in anoxic aquifers, where for example *Thermodesulfovibrio* are more dominant. We mostly detected these anaerobic Nitrospirota lineages in hypoxic Kurikka groundwaters. This aligns with findings of Mosley et al. (2024) showing that the majority of Nitrospirota genomes recovered from aquifers possess metabolic traits linked to anaerobic nitrogen and sulphur transformations. With nitrate below detection limit (0.5mg/L) at all sites, the geochemistry testifies the post-denitrification conditions in the redox ladder, and likely Nitrospirae in Kurikka groundwaters are depending on other metabolic pathways than nitrate oxidation. No microbial community data is available from KUU19 but it was the only sample that had a nitrate concentration above the detection limit (Supplementary Table 1). This is likely explained by the agricultural activity in the area. KUU19 site is influenced by intensive test pumping (700-1000 m3/day) from a nearby production well, causing more dynamic groundwater flow compared to natural conditions likely explaining the anomalies seen in the KUU19 sample.

Low biomass in groundwater samples resulted in very small amounts of recoverable DNA, which is the probable cause for unsuccessful retrieval of sequencing data from KUU19, MIHP6 and HÄJY11. Additionally, only bacterial community from LOHI30 could be retrieved. Archaea are typically less abundant in groundwater environments compared to bacteria, and with low amount of DNA to begin with here, sequencing has missed the archaea. Similarly, the abundance of fungal cells in groundwaters might be much lower than bacteria, and additionally, fungi may also require more rigorous cell-disruption steps during extraction compared to prokaryotes, causing a reduced fungal DNA yield and unsuccessful sequencing here. In addition, the filters used here were not specifically designed for this purpose, so methodological limitations may have led to inefficient biomass elution and low final DNA recovery. One potential reason for low DNA recovery could also be organic compounds interfering with the DNA extraction, as we detected a brownish colour emerging to the filters while pumping the groundwater through.

4.3 Usability of tested tracers in complex aquifers

The tracers applied in this study provide valuable initial insights into the Kurikka buried valley aquifer system and demonstrate their potential for supporting further hydrogeological characterization, even though some limitations were identified. Despite the challenges brought by observation wells with long screens (12 to 30 m) and single-campaign sampling, the combination of isotopic, residence time and microbial approaches produced a broad and informative view of groundwater processes in a geologically complex setting.

Water stable isotopes proved effective in establishing that sampled groundwaters do not contain a surface water component. Their clear and consistent signatures form a robust baseline for tracing future hydraulic changes influenced by extensive groundwater extraction. Although spatial variability exists, strontium isotope signatures provide an important reference for identifying mixing of groundwaters in the Kurikka buried valley aquifer system as pumping tests continue and more sampling campaigns are carried out.

This excludes the seasonal changes in redox conditions that might affect the S isotopic compositions, or the seasonal changes in the isotopic compositions of water stable isotopes in precipitation. Furthermore, the sampling was done from only 10 locations. For a more complete hydrogeochemical assessment of the end-member compositions more sampling around the study area can be recommended and will be published as results of the additional hydrogeological investigations of the study area.

The applicability of different environmental tracers for groundwater age dating was assessed in this study. While CFCs, noble gases and SF6 were rendered unreliable by tracer degradation, contamination, excess air and in-situ production process, the 3H-3He method yielded robust age estimates for selected samples, despite elevated radiogenic helium concentrations. These results underline the need for site-specific tracer assessment and confirm that meaningful groundwater residence times can be derived even in complex hydrogeological settings. An advantage would be observation wells with short filter screen of for example ~2m. Tritium with low detection limit, achievable with the ^{3}He ingrowth method, as well as radiocarbon emerge as promising options for improving residence time estimates and identification of old groundwater components in the system.

Microbial community profiling revealed differences between the sites. However, many phyla and orders are shared among all sites, this taxonomic overlap limits their use as standalone tracers. Greater resolution might be achieved by examining lower taxonomic levels, and while partial 16S rRNA gene sequencing typically lacks species-level accuracy (Johnson et al. 2019), this can be circumvented by sequencing the whole 16S rRNA gene using long-read approaches. Specific taxa, such as *Hydrogenophaga*, show promise as indicators of specific environments like bedrock groundwater. The microbial community diversity also tracked well with groundwater age, supporting their use as complementary tracers of subsurface environments.

Conclusions

This study highlighted the unique characteristics of deep groundwaters found in the buried valley aquifer system in Kurikka, focusing on combined isotopic, residence time and microbial tracer analyses. Together, these approaches provide a robust, first-order understanding of the groundwater system structure, connectivity and functioning prior to extensive groundwater extraction. The findings indicate that the groundwater in the Paloluoma Valley and Harjankylä in the Kyrönjoki Valley appear to be younger compared to the other areas in the Kyrönjoki Valley. This is attributed to the proximity of recharge areas, an important observation for groundwater management, as it indicates areas where the system may respond more rapidly to pumping and seasonal variations. Isotopic compositions of oxygen and hydrogen confirm that no surface water component is present in the groundwater samples. Strontium isotopes reflect local mineralogy and establish a reference for future mixing studies, assuming the pumping tests will influence the hydraulic connections in the aquifer system. Isotopic evidence suggests hydraulic connectivity between the lowermost aquifer and the underlying fractured bedrock. Although the extent of the fractured bedrock as a water reservoir remains unclear, the isotope data indicate that interactions between the two units are likely. The study shows that several environmental tracers for groundwater residence time determination fail under the investigated conditions. However, the 3H-3He method remained applicable for samples with measurable tritium. Groundwater residence time estimates indicate predominantly modern water. This further supports the interpretation that where mixing occurs between water from the bedrock surface and the lowermost unconsolidated aquifer, the groundwater flow within the fractured bedrock is likely relatively unrestricted.

The results demonstrate that groundwater microbial communities are diverse and vary distinctly between the studied sites along the aquifer system in Kurikka. The bedrock-related microbial community exhibits special features compared to the groundwaters from shallower unconsolidated aquifers. The site at a more superficial esker system with relatively young groundwater hosted the most diverse prokaryotic community, whereas bedrock with the oldest waters supported the lowest diversity. This age-dependent trend is consistent with geochemical expectations for deep, isolated groundwater environments. Sulphur isotope compositions in the groundwater further reinforce the link between geochemistry and microbiology.

Because this study was conducted prior to large-scale groundwater extraction, the geochemical, isotopic, residence time and microbial data presented here form an essential baseline. Thus, each sampling site can serve as an endmember against which future changes can be evaluated. Establishing these initial conditions is important for detecting shifts in e.g., geochemical pathways or microbial activity that may arise as the aquifer system responds to stress.

Although one of the aims of this study was to assess whether a combined multitracer approach could resolve hydraulic connectivity and flow dynamics within this complex buried valley system, the present dataset provides only preliminary indications rather than definitive evidence. Isotopic, microbial and sulphur-isotope patterns point to potential zones of interaction between aquifer units, but limitations in spatial coverage, well construction and temporal resolution prevent firm conclusions regarding flow paths or mixing processes. Instead, the results identify where such connections may exist and

highlight which tracers are most promising for future high-resolution investigations. The multitracer framework establishes the methodological foundation for future studies designed to rigorously test this hypothesis under expanded sampling and pumping conditions.

Further research is still required to clarify outstanding questions, including the extent of hydraulic conductivity between different parts of the aquifer and the fractured bedrock underneath, and its role as a potential flow path. Nonetheless, the insights gained here provide a foundation for understanding and managing groundwater resources. These results serve as key references for interpreting test pumping data and future investigations in the unique Kurikka buried valley aquifer system.

Author contributions

LP, JI and MAP jointly conceptualized the idea, conducted the investigation, analysed the data and wrote and edited the original manuscript. NP took part in conceptualization, provided funding and resources and commented on the original manuscript. JS took part in investigation and participated in the revision of the manuscript. MM took part in investigation and commented on the original manuscript. AH took part in conceptualization, investigation and analysis of the data and writing and editing of the original manuscript. TP provided resources and participated in conceptualization of the idea. IM provided funding and resources and mentoring during idea conceptualization.

The authors declare that they have no conflict of interest.

Data availability

All data is available either in the publication, in its supplementary material, or NCBI's SRA under BioProject PRJNA1270735 (sequence data).

Acknowledgements

Arto Pullinen, Salla Valpola, Vaula Lukkarinen and Kim Wennman are thanked for their help during the fieldwork. Yann Lahaye, Mia Tiljander, Meiru Zhou and Katariina Issukka at the GTK laboratory, and the personnel of laboratory of water microbiology at THL are acknowledged for their contribution to laboratory analyses. Nina Hendriksson and Aleksi Tuunainen are thanked for the helpful comments and aid with the characteristics of groundwater wells. Authors also thank the Kurikka Aquifer project consortium partners: Kurikan Vesihuolto Oy, Vaasan Vesi, and ELY Centre for South Ostrobothnia (EPOELY) for funding and resources for the project. We are also sincerely thankful to all private landowners who allowed access to the sampling sites. During the preparation of this manuscript the authors used Microsoft Copilot to improve language and readability. After using this tool, the authors reviewed and edited the content as needed and take full responsibility for the content of the publication.

References

Abarenkov, K., Nilsson, R. H., Larsson, K. H., et al. (2024). The UNITE database for molecular identification and taxonomic communication of fungi and other eukaryotes: sequences, taxa and classifications reconsidered. Nucleic Acids Research, 52(D1), D791–D797. https://doi.org/10.1093/NAR/GKAD1039

Andersen, K. S., Kirkegaard, R. H., Karst, S. M., & Albertsen, M. (2018). ampvis2: an R package to analyse and visualise 16S rRNA amplicon data. https://doi.org/10.1101/299537

Appelo, C.A.J., Postma, D. (2004). Geochemistry, groundwater and pollution, 2nd Edition. CRC press, A.A. Balkema Publishers, Leiden, The Netherlands. 649 p.

Apprill, A., McNally, S., Parsons, R., & Weber, L. (2015). Minor revision to V4 region SSU rRNA 806R gene primer greatly increases detection of SAR11 bacterioplankton. Aquatic Microbial Ecology, 75(2), 129–137. https://doi.org/10.3354/ame01753

Ben Maamar, S., Aquilina, L., Quaiser, A., Pauwels, H., Michon-Coudouel, S., Vergnaud-Ayraud, V., Labasque, T., Roques, C., Abbott, B. W., & Dufresne, A. (2015). Groundwater isolation governs chemistry and microbial community structure along hydrologic flowpaths. Frontiers in Microbiology, 6(DEC), 1–13. https://doi.org/10.3389/fmicb.2015.01457

Bethke, C. M., Sanford, R. a., Kirk, M. F., Jin, Q., & Flynn, T. M. (2011). The thermodynamic ladder in geomicrobiology. American Journal of Science, 311(3), 183–210. https://doi.org/10.2475/03.2011.01

Bullen, T. D., Krabbenhoft, D. P., and Kendall, C.: Kinetic and mineralogic controls on the evolution of groundwater chemistry and 87Sr/86Sr in a sandy silicate aquifer, northern Wisconsin, USA, Geochim. Cosmochim. Acta, 60, 1807–1821, https://doi.org/10.1016/0016-7037(96)00052-X, 1996.

Bärenstrauch, M., Vanhove, A. S., Allégra, S., Peuble, S., Gallice, F., Paran, F., Lavastre, V., & Girardot, F. (2022). Microbial diversity and geochemistry of groundwater impacted by steel slag leachates. Science of The Total Environment, 843, 156987. https://doi.org/10.1016/J.SCITOTENV.2022.156987

Callahan, B. J., McMurdie, P. J., Rosen, M. J., Han, A. W., Johnson, A. J. A., & Holmes, S. P. (2016). DADA2: High resolution sample inference from Illumina amplicon data. Nature Methods, 13(7), 581. https://doi.org/10.1038/NMETH.3869

Carreira, P. M. and Marques, J. M.: The Use of Environmental Isotopes in Hydrogeology, Water 2024, Vol. 16, Page 914, 16, 914, https://doi.org/10.3390/W16070914, 2024.

Castelle, C. J., Wrighton, K. C., Thomas, B. C., Hug, L. A., Brown, C. T., Wilkins, M. J., Frischkorn, K. R., Tringe, S. G., Singh, A., Markillie, L. M., Taylor, R. C., Williams, K. H., & Banfield, J. F. (2015). Genomic expansion of domain archaea highlights roles for organisms from new phyla in anaerobic carbon cycling. Current Biology, 25(6), 690–701. https://doi.org/10.1016/j.cub.2015.01.014

Cauquoin, A., Fourré, É., Landais, A., Okazaki, A., & Yoshimura, K. (2024). Modeling natural tritium in precipitation and its dependence on decadal solar activity variations using the atmospheric general circulation model MIROC5-iso. J Geophys Res: Atmospheres, 129, e2023JD039745. https://doi.org/10.1029/2023JD039745

Chaudhari, N. M., Overholt, W. A., Figueroa-Gonzalez, P. A., Taubert, M., Bornemann, T. L. V., Probst, A. J., Hölzer, M., Marz, M., & Küsel, K. (2021). The economical lifestyle of CPR bacteria in groundwater allows little preference for environmental drivers. Environmental Microbiomes, 16(1), 1–18. https://doi.org/10.1186/S40793-021-00395-W/FIGURES/8

Clark, I. and Fritz, P. (1997). Environmental Isotopes in Hydrogeology. CRC press, Taylor & Francis Group, Boca Raton, FL, U.S. 328 p.

Clark, I. (2015). Groundwater geochemistry and isotopes. CRC press, Taylor & Francis Group, Boca Raton, FL, U.S. 438 p.

Cook, P.G., Solomon, D.K. (1997). Recent advances in dating young groundwater: chlorofluorocarbons, ^{3}H ^{3}He and ^{85}Kr. J Hydrol 191:245–265. https://doi.org/10.1016/S0022-1694(96)03051-X

Daims, H., Lebedeva, E. V., Pjevac, P., Han, P., Herbold, C., Albertsen, M., Jehmlich, N., Palatinszky, M., Vierheilig, J., Bulaev, A., Kirkegaard, R. H., Von Bergen, M., Rattei, T., Bendinger, B., Nielsen, P. H., & Wagner, M. (2015). Complete nitrification by Nitrospira bacteria. Nature, 528(7583), 504–509. https://doi.org/10.1038/nature16461

Divine, C. E. and McDonnell, J. J.: The future of applied tracers in hydrogeology, Hydrogeol. J., 13, 255–258, https://doi.org/10.1007/S10040-004-0416-3/METRICS, 2005.

Flynn, T. M., Sanford, R. a, Ryu, H., Bethke, C. M., Levine, A. D., Ashbolt, N. J., & Santo Domingo, J. W. (2013). Functional microbial diversity explains groundwater chemistry in a pristine aquifer. BMC Microbiology, 13(1). https://doi.org/10.1186/1471-2180-13-146

Freeze, R.A., Cherry, J.A. (1979). Groundwater. Prentice-Hall, Hoboken, New Jersey, U.S. 604 p.

Gantner, S., Andersson, A. F., Alonso-Sáez, L., & Bertilsson, S. (2011). Novel primers for 16S rRNA-based archaeal community analyses in environmental samples. Journal of Microbiological Methods, 84(1), 12–18. https://doi.org/10.1016/j.mimet.2010.10.001

Griebler, C., & Lueders, T. (2009). Microbial biodiversity in groundwater ecosystems. Freshwater Biology, 54(4), 649–677. https://doi.org/10.1111/j.1365-2427.2008.02013.x

Grönwall, J. and Danert, K. (2020). Regarding Groundwater and Drinking Water Access through A Human Rights Lens: Self-Supply as A Norm, Water 2020, Vol. 12, Page 419, 12, 419, https://doi.org/10.3390/W12020419

Hall, A. M., Putkinen, N., Hietala, S., Lindsberg, E., & Holma, M. (2021). Ultra-slow cratonic denudation in Finland since 1.5 Ga indicated by tiered unconformities and impact structures. Precambrian Research, 352, 106000. https://doi.org/10.1016/J.PRECAMRES.2020.106000

Hallbeck, L., & Pedersen, K. (2014). The family Gallionellaceae. In E. Rosenberg, E. F. DeLong, S. Lory, E. Stackebrandt, & F. Thompson (Eds.), The Prokaryotes: Alphaproteobacteria and Betaproteobacteria (pp. 853–858). Springer. https://doi.org/10.1007/978-3-642-30197-1_398

Harrison, A. G. and Thode, H. G. (1958). Sulphur Isotope Abundances in Hydrocarbons and Source Rocks of Uinta Basin, Utah, Am. Assoc. Pet. Geol. Bull., 42, 2642–2649, https://doi.org/10.1306/0BDA5C00-16BD-11D7-8645000102C1865D, 1958.

Herlemann, D. P., Labrenz, M., Jürgens, K., Bertilsson, S., Waniek, J. J., & Andersson, A. F. (2011). Transitions in bacterial communities along the 2000 km salinity gradient of the Baltic Sea. The ISME Journal, 5(10), 1571–1579. https://doi.org/10.1038/ismej.2011.41

Hoover, R. L., Keffer, J. L., Polson, S. W., & Chan, C. S. (2023). Gallionellaceae pangenomic analysis reveals insight into phylogeny, metabolic flexibility, and iron oxidation mechanisms. MSystems, 8(6). https://doi.org/10.1128/MSYSTEMS.00038-23/SUPPL_FILE/MSYSTEMS.00038-23-S0002.XLSX

Hou, J., Chen Yang, C., Wang, F. (2025) Carbon metabolic versatility underpins *Bathyarchaeia* ecological significance across the global deep subsurface. *The ISME Journal*, 19, wraf259. https://doi.org/10.1093/ismejo/wraf259

Hutchins, B.T., Engel, A.S., Nowlin, W.H., Schwartz, B.F. (2016) Chemolithoautotrophy supports macroinvertebrate food webs and affects diversity and stability in groundwater communities. Ecology. 97:1530-42. doi: 10.1890/15-1129.1. PMID: 27459783.

Ikonen, J., Rauhala, A., Tuomela, A., Postila, H., Kumpula, T., Korpelainen, P., Pietilä, R., Valta, R. O., Lerssi, J., Panttila, H., and Korkka-Niemi, K. (2025): Combining UAS-TIR and GEM-2 Techniques for Focused Water Sampling and Isotope Geochemical Analysis at Two Mine Sites in Northern Finland, Mine Water Environ., 44, 177–198, https://doi.org/10.1007/S10230-024-01020-1/FIGURES/13

Inkinen, J., Jayaprakash, B., Siponen, S., Hokajärvi, A. M., Pursiainen, A., Ikonen, J., Ryzhikov, I., Täubel, M., Kauppinen, A., Paananen, J., Miettinen, I. T., Torvinen, E., Kolehmainen, M., & Pitkänen, T. (2019). Active eukaryotes in drinking water distribution systems of ground and surface waterworks. Microbiome, 7(1), 1–17. https://doi.org/10.1186/S40168-019-0715-5/FIGURES/7

Jaunat, J., Huneau, F., Dupuy, A., et al. (2012). Hydrochemical data and groundwater dating to infer differential flowpaths through weathered profiles of a fractured aquifer. Appl Geochem 27:2053–2067

Johnson, J.S., Spakowicz, D.J., Hong, B.Y. et al. (2019). Evaluation of 16S rRNA gene sequencing for species and strain-level microbiome analysis. Nat Commun 10, 5029 https://doi.org/10.1038/s41467-019-13036-1

Johnson, T. D., Belitz, K., Kauffman, L. J., Watson, E., and Wilson, J. T. (2022) Populations using public-supply groundwater in the conterminous U.S. 2010; Identifying the wells, hydrogeologic regions, and hydrogeologic mapping units, Sci. Total Environ., 806, 150618, https://doi.org/10.1016/J.SCITOTENV.2021.150618

Kaislaniemi, L. (2011). Estimating the distribution of strontium isotope ratios 87Sr/86Sr in the Precambrian of Finland, Bull. Geol. Soc. Finl., https://doi.org/10.17741/bgsf/83.2.002

Kaplan, I. R. and Rittenberg, S. C. (1964). Microbiological fractionation of sulphur isotopes., J. Gen. Microbiol., 34, 195–212, https://doi.org/10.1099/00221287-34-2-195/CITE/REFWORKS

Kato, S., & Ohkuma, M. (2021). A Single Bacterium Capable of Oxidation and Reduction of Iron at Circumneutral pH. Microbiology Spectrum, 9(1). https://doi.org/10.1128/SPECTRUM.00161-21/SUPPL_FILE/SPECTRUM00161-21_SUPP_1_SEQ4.PDF

Kauppinen, A., Pitkänen, T., Al-Hello, H., Maunula, L., Hokajärvi, A.-M., Rimhanen-Finne, R., & Miettinen, I. T. (2019). Two Drinking Water Outbreaks Caused by Wastewater Intrusion Including Sapovirus in Finland. International Journal of Environmental Research and Public Health, 16(22), 4376. https://doi.org/10.3390/ijerph16224376

Kietäväinen, R., Ahonen, L., Kukkonen, I. T., Hendriksson, N., Nyyssönen, M., and Itävaara, M. (2013). Characterisation and isotopic evolution of saline waters of the Outokumpu Deep Drill Hole, Finland – Implications for water origin and deep terrestrial biosphere, *Appl. Geochemistry,* 32, 37–51, https://doi.org/10.1016/J.APGEOCHEM.2012.10.013.

Kietäväinen, R., Ahonen, L., Kukkonen, I. T., Niedermann, S., Wiersberg, T. (2014). Noble gas residence times of saline waters within crystalline bedrock, Outokumpu Deep Drill Hole, Finland. *Geochim Cosmochim Acta*, 145, 159–174. https://doi.org/10.1016/j.gca.2014.09.012

Kipfer, R., Aeschbach-Hertig, W., Peeters, F., Stute, M. (2002). Noble Gases in Lakes and Ground Waters. *Rev Mineral Geochem* 2002;47 (1): 615–700. doi: https://doi.org/10.2138/rmg.2002.47.14

Kløve, B., Kvitsand, H.M.L., Pitkänen, T., Gunnarsdottir, M. J, Gaut, S., Gardarsson, S. M., Rossi, P. M., Miettinen, I. (2017). Overview of groundwater sources and water-supply systems, and associated microbial pollution, in Finland, Norway and Iceland. *Hydrogeol J* **25**, 1033–1044. https://doi.org/10.1007/s10040-017-1552-x

Lahtinen, R., Huhma, H., Sipilä, P., Vaarma, M. (2017). Geochemistry, U-Pb geochronology and Sm-Nd data from the Paleoproterozoic Western Finland supersuite—a key component in the coupled Bothnian oroclines. *Precambrian Research*, 299, 264–281. https://doi.org/10.1016/j.precamres.2017.07.02

Lee, J. H., Lee, B. J., & Unno, T. (2018). Bacterial Communities in Ground-and Surface Water Mixing Zone Induced by Seasonal Heavy Extraction of Groundwater. Geomicrobiology Journal, 35(9), 768–774. https://doi.org/10.1080/01490451.2018.1468834

Lever, M. A. (2012). Acetogenesis in the energy-starved deep biosphere - a paradox? Frontiers in Microbiology, 2, 284. https://doi.org/10.3389/fmicb.2011.00284; 10.3389/fmicb.2011.00284

Liu, X., Li, M., Castelle, C. J., Probst, A. J., Zhou, Z., Pan, J., Liu, Y., Banfield, J. F., & Gu, J. D. (2018). Insights into the ecology, evolution, and metabolism of the widespread Woesearchaeotal lineages. Microbiome, 6(1), 102-. https://doi.org/10.1186/S40168-018-0488-2/FIGURES/6

Luef, B., Frischkorn, K. R., Wrighton, K. C., Holman, H. N., Birarda, G., Thomas, B. C., Singh, A., Williams, K. H., Siegerist, C. E., Tringe, S. G., Downing, K. H., Comolli, L. R., & Banfield, J. F. (2015). Diverse uncultivated ultra-small bacterial cells in groundwater. Nature Communications, *6*, 1–8. https://doi.org/10.1038/ncomms7372

Luoma, S., Okkonen, J., Korkka-Niemi, K., Hendriksson, N., and Paalijärvi, M. (2024) Characterization of Groundwater Geochemistry in an Esker Aquifer in Western Finland Based on Three Years of Monitoring Data, Water 2024, 16, 3301, https://doi.org/10.3390/W16223301, 2024.

Lyons, K. J., Hokajärvi, A.-M., Ikonen, J., Kauppinen, A., Miettinen, I. T., Pitkänen, T., Rossi, P. M., & Kujala, K. (2021). Surface Water Intrusion, Land Use Impacts, and Bacterial Community Composition in Shallow Groundwater Wells Supplying Potable Water in Sparsely Populated Areas of a Boreal Region. https://doi.org/10.1128/Spectrum.00179-21

Martin, M. (2011). Cutadapt removes adapter sequences from high-throughput sequencing reads. EMBnet.Journal, 17(1), 10–12. https://doi.org/10.14806/EJ.17.1.200

Massmann, G., Sültenfuß, J., Dünnbier, U., et al. (2008). Investigation of groundwater residence times during bank filtration in Berlin: a multi-tracer approach. Hydrol Process 22:788–801. https://doi.org/10.1002/hyp.6649

Mayer, A., Sültenfuß, J., Travi, Y., Rebeix, R., Purtschert, R., Claude, C., Le Gal La Salle, C., Miche, H., und Conchetto, E. (2014). A multi-tracer study of groundwater origin and transit-time in the aquifers of the Venice region (Italy). Appl. Geochem., doi:10.1016/j.apgeochem.2013.10.009.

McMurdie, P. J., & Holmes, S. (2013). Phyloseq: An R Package for Reproducible Interactive Analysis and Graphics of Microbiome Census Data. PLoS ONE, 8(4). https://doi.org/10.1371/journal.pone.0061217

Merino, N., Jackson, T. R., Campbell, J. H., Kersting, A. B., Sackett, J., Fisher, J. C., Bruckner, J. C., Zavarin, M., Hamilton-Brehm, S. D., & Moser, D. P. (2022). Subsurface microbial communities as a tool for characterizing regional-scale groundwater flow. Science of The Total Environment, 842, 156768. https://doi.org/10.1016/J.SCITOTENV.2022.156768

Meyzonnat, G., Musy, S., Corcho-Alvarado, J.A., et al. (2023). Age distribution of groundwater in fractured aquifers of the St. Lawrence Lowlands (Canada) determined by environmental tracers ($^{3}H/^{3}He$, ^{85}Kr, SF_6, CFC-12, ^{14}C). Hydrogeol J 31:2139–2157. https://doi.org/10.1007/s10040-023-02671-0

Momper, L., Jungbluth, S. P., Lee, M. D., & Amend, J. P. (2017). Energy and carbon metabolisms in a deep terrestrial subsurface fluid microbial community. The ISME Journal, 11(10), 2319–2333. https://doi.org/10.1038/ismej.2017.94

Mosley, O. E., Gios, E., & Handley, K. M. (2024). Implications for nitrogen and sulphur cycles: phylogeny and niche-range of Nitrospirota in terrestrial aquifers. ISME Communications, 4(1), 47. https://doi.org/10.1093/ISMECO/YCAE047

National Ground Water Association: https://www.ngwa.org/what-is-groundwater/About-groundwater, last access 1 April 2025

Négrel, P., Casanova, J., Blomqvist, R., Kaija, J., and Frape, S. (2003). Strontium isotopic characterization of the Palmottu hydrosystem (Finland): water–rock interaction and geochemistry of groundwaters, Geofluids, 3, 161–175, https://doi.org/10.1046/J.1468-8123.2003.00056.X

Négrel, P., Pauwels, H., and Chabaux, F. (2018). Characterizing multiple water-rock interactions in the critical zone through Sr-isotope tracing of surface and groundwater, Appl. Geochemistry, 93, 102–112, https://doi.org/10.1016/J.APGEOCHEM.2018.04.006

Oksanen, J., Simpson, G. L., Blanchet, F. G., Kindt, R., Legendre, P., Minchin, P. R., O'Hara, R. B., Solymos, P., Stevens, M. H. H., Szoecs, E., Wagner, H., Barbour, M., Bedward, M., Bolker, B., Borcard, D., Borman, T., Carvalho, G., Chirico,

M., De Caceres, M., … Weedon, J. (2025). vegan: Community Ecology Package (Version 2.8-0). https://doi.org/10.32614/CRAN.package.vegan

Onac, B. P., Wynn, J. G., and Sumrall, J. B. (2011). Tracing the sources of cave sulfates: a unique case from Cerna Valley, Romania, Chem. Geol., 288, 105–114, https://doi.org/10.1016/J.CHEMGEO.2011.07.006

Osenbrück, K., Fiedler, S., Knöller, K., et al. (2006). Timescales and development of groundwater pollution by nitrate in drinking water wells of the Jahna-Aue, Saxonia, Germany. Water Resour Res 42:

Paris, G., A.L. Sessions, A.V. Subhas, and J.F. Adkins (2013). MC-ICP-MS measurement of δ34S and Δ33S in small amounts of dissolved sulfate. Chemical Geology 345: 50-61

Perez-Molphe-Montoya, E., Küsel, K. and Overholt, W. A. (2022). Redefining the phylogenetic and metabolic diversity of phylum Omnitrophota. https://doi.org/10.1111/1462-2920.16170

Poghosyan, L., Koch, H., Lavy, A., Frank, J., van Kessel, M. A. H. J., Jetten, M. S. M., Banfield, J. F., & Lücker, S. (2019). Metagenomic recovery of two distinct comammox Nitrospira from the terrestrial subsurface. Environmental Microbiology, 21(10), 3627–3637. https://doi.org/10.1111/1462-2920.14691

Porru, M. C., Arras, C., Biddau, R., Cidu, R., Lobina, F., Podda, F., Wanty, R., and Da Pelo, S. (2024) Assessing Recharge Sources and Seawater Intrusion in Coastal Groundwater: A Hydrogeological and Multi-Isotopic Approach, Water (Switzerland), 16, 1106, https://doi.org/10.3390/W16081106/S1

Purkamo, L., Bomberg, M., Kietäväinen, R., Salavirta, H., Nyyssönen, M., Nuppunen-Puputti, M., Ahonen, L., Kukkonen, I., & Itävaara, M. (2016). Microbial co-occurrence patterns in deep Precambrian bedrock fracture fluids. Biogeosciences, 13(10). https://doi.org/10.5194/bg-13-3091-2016

Purkamo, L., Bomberg, M., Nyyssönen, M., Kukkonen, I., Ahonen, L., Kietäväinen, R., & Itävaara, M. (2013). Dissecting the deep biosphere: Retrieving authentic microbial communities from packer-isolated deep crystalline bedrock fracture zones. FEMS Microbiology Ecology, 85(2), 324–337. https://doi.org/10.1111/1574-6941.12126

Purkamo, L., Kietäväinen, R., Miettinen, H., Sohlberg, E., Kukkonen, I., Itävaara, M., & Bomberg, M. (2018). Diversity and functionality of archaeal, bacterial and fungal communities in deep Archaean bedrock groundwater. FEMS Microbiology Ecology, 94(8), 1–14. https://doi.org/10.1093/femsec/fiy116

Putkinen, N., Ruskeeniemi, T., Hall, A., Silvennoinen, S., Skyttä, P., Lefebvre, R., Lunkka, J. P., Malinowski, M., Lindsberg, E., Åberg, A., Laakso, V., Koskela, E., Heinonen, S., Eyles, N. & Ross, M. (2025). Characterization and development of a buried-valley aquifer system in western Finland: development from the Proterozoic to the Quaternary. *In review*, Quaternary International.

Quast, C., Pruesse, E., Yilmaz, P., Gerken, J., Schweer, T., Yarza, P., Peplies, J., & Glöckner, F. O. (2013). The SILVA ribosomal RNA gene database project: Improved data processing and web-based tools. Nucleic Acids Research, 41(D1), D590-6. https://doi.org/10.1093/nar/gks1219

Quince, C., Lanzen, A., Davenport, R. J., & Turnbaugh, P. J. (2011). Removing Noise From Pyrosequenced Amplicons. BMC Bioinformatics, 12(1), 38. https://doi.org/10.1186/1471-2105-12-38

R Core Team. (2024). R: A language and environment for statistical computing (https://www.R-project.org/). R Foundation for Statistical Computing.

Rashid, A.B. (2022). Towards Quantifying Groundwater Resources of the Paloluoma Buried Bedrock Valley in Western Finland with Groundwater Modelling. Master of Science, University of Waterloo.

Retter, A., Griebler, C., Nilsson, R. H., Haas, J., Birk, S., Breyer, E., Baltar, F., & Karwautz, C. (2024). Metabarcoding reveals ecologically distinct fungal assemblages in river and groundwater along an Austrian alpine to lowland gradient. FEMS Microbiology Ecology, 100(11), 139. https://doi.org/10.1093/FEMSEC/FIAE139

Rosenberg, E., DeLong, E. F., Lory, S., Stackebrandt, E., & Thompson, F. (Eds.). (2014). The Prokaryotes. Springer Berlin Heidelberg. https://doi.org/10.1007/978-3-642-38954-2

Ruff, S. E., Humez, P., de Angelis, I. H., Diao, M., Nightingale, M., Cho, S., Connors, L., Kuloyo, O. O., Seltzer, A., Bowman, S., Wankel, S. D., McClain, C. N., Mayer, B., & Strous, M. (2023). Hydrogen and dark oxygen drive microbial productivity in diverse groundwater ecosystems. Nature Communications 2023 14:1, 14(1), 1–17. https://doi.org/10.1038/s41467-023-38523-4

Ruuska E., Skyttä P., Putkinen N., Valjus T. (2023). Contribution of bedrock structures to the bedrock surface topography and groundwater flow systems within deep glaciofluvial aquifers in Kurikka, Western Finland. Earth Surf. Processes Landforms 48, 2039-2056. https://doi.org/10.1002/esp.5602.

Samborska-Goik, K. and Bottrell, S. (2025). Bayesian modelling of sulphate isotopic composition in pristine, contaminated, and experimental environments for investigating microbial bacterial reduction, J. Hydrol., 652, 132662, https://doi.org/10.1016/J.JHYDROL.2024.132662

Schwab, V. F., Herrmann, M., Roth, V. N., Gleixner, G., Lehmann, R., Pohnert, G., Trumbore, S., Küsel, K., & Totsche, K. U. (2017). Functional diversity of microbial communities in pristine aquifers inferred by PLFA- and sequencing-based approaches. Biogeosciences, 14(10), 2697–2714. https://doi.org/10.5194/BG-14-2697-2017

Shand, P., Darbyshire, D. P. F., Love, A. J., and Edmunds, W. M. (2009). Sr isotopes in natural waters: Applications to source characterisation and water–rock interaction in contrasting landscapes, Appl. Geochemistry, 24, 574–586, https://doi.org/10.1016/J.APGEOCHEM.2008.12.011

Shapiro, S. D, Rowe, G., Schlosser, P., Andrea Ludin, A., and Stute, M. (1998). Tritium–Helium 3 Dating under Complex Conditions in Hydraulically Stressed Areas of a Buried-valley Aquifer. *Water Resources Research* 34, 1165–80. https://doi.org/10.1029/97WR03322

Simler, R. (2012). Software "Diagrammes," Laboratoire d'Hydrologie d'Avignon, Université d'Avignon et pays du Vaucluse, France. http://www.lha.univ-avignon.fr

Sohlberg, E., Bomberg, M., Miettinen, H., Nyyssönen, M., Salavirta, H., Vikman, M., & Itävaara, M. (2015). Revealing the unexplored fungal communities in deep groundwater of crystalline bedrock fracture zones in Olkiluoto, Finland. Frontiers in Microbiology, 6(JUN), 1–11. https://doi.org/10.3389/fmicb.2015.00573

Solomon, D. K., & Gilmore, T. E. (2024). Age dating young groundwater: How to determine groundwater age from environmental tracer data. The Groundwater Project. https://doi.org/10.21083/LIIU2727

Sonier, D.N., Duran, N.L. Smith, G.B. (1994). Dechlorination of Trichlorofluoromethane (CFC-11) by Sulfate-Reducing Bacteria from an Aquifer Contaminated with Halogenated Aliphatic Compounds., Appl. Env.Microbiol. 60, 4567-4572

Stroeven A. P., Hättestrand, C., Kleman J., Heyman, J., Fabel, D., Fredin, O., Goodfellow, B. W., Harbor J. M., Jansen J. D., Olsen, L., Caffee M. W., Fink, D., Lundqvist, J., Rosqvist, G. C., Strömberg, B., Jansson, K. N. (2016) Deglaciation of Fennoscandia. Quaternary Science Reviews, 147, 91-121. http://dx.doi.org/10.1016/j.quascirev.2015.09.016

Suominen, S., Dombrowski, N., Sinninghe Damsté, J. S., & Villanueva, L. (2021). A diverse uncultivated microbial community is responsible for organic matter degradation in the Black Sea sulphidic zone. Environmental Microbiology, 23(6), 2709–2728. https://doi.org/10.1111/1462-2920.14902

Sültenfuß, J., Roether, W., Rhein, M. (2009). The Bremen mass spectrometric facility for the measurement of helium isotopes, neon, and tritium in water. Isotopes Environ Health Stud 45:83–95. https://doi.org/10.1080/10256010902871929

Tan, S., Liu, J., Fang, Y., Hedlund, B. P., Lian, Z. H., Huang, L. Y., Li, J. T., Huang, L. N., Li, W. J., Jiang, H. C., Dong, H. L., & Shu, W. S. (2019). Insights into ecological role of a new deltaproteobacterial order Candidatus Acidulodesulfobacterales by metagenomics and metatranscriptomics. The ISME Journal 2019 13:8, 13(8), 2044–2057. https://doi.org/10.1038/s41396-019-0415-y

Visser, A., Broers, H.P., Purtschert, R., et al. (2013). Groundwater age distributions at a public drinking water supply well field derived from multiple age tracers (^{85}Kr, ^{3}H/^{3}He, and ^{39}Ar). Water Resour Res 49:7778–7796

de Vries A, Ripley BD (2024). ggdendro: Create Dendrograms and Tree Diagrams Using 'ggplot2'. R package version 0.2.0, https://andrie.github.io/ggdendro/

White, T. J., Bruns, S., Lee, S., & Taylor, J. (1990). Amplification and direct sequencing of fungal ribosomal RNA genes for phyologenetics.pdf. In PCR Protocols: A Guide to Methods and Applications (pp. 315–322). https://doi.org/citeulike-article-id:671166

Wickham H (2016). ggplot2: Elegant Graphics for Data Analysis. Springer-Verlag New York. ISBN 978-3-319-24277-4, https://ggplot2.tidyverse.org.

Wickham, H., François, R., Henry, L., Müller, K., & Vaughan, D. (2026). *dplyr: A Grammar of Data Manipulation (Version 1.2.0)*. https://dplyr.tidyverse.org

Wilke, C. O. (2025). *cowplot: Streamlined Plot Theme and Plot Annotations for "ggplot2". R package version 1.2.0,*. https://wilkelab.org/cowplot/

Williams, T. J., Allen, M. A., Berengut, J. F., & Cavicchioli, R. (2021). Shedding Light on Microbial "Dark Matter": Insights Into Novel Cloacimonadota and Omnitrophota From an Antarctic Lake. Frontiers in Microbiology, 12, 741077. https://doi.org/10.3389/FMICB.2021.741077/XML/NLM

Yilmaz, P., Parfrey, L. W., Yarza, P., Gerken, J., Pruesse, E., Quast, C., Schweer, T., Peplies, J., Ludwig, W., & Glöckner, F. O. (2014). The SILVA and & All-species Living Tree Project (LTP); taxonomic frameworks. Nucleic Acids Research, 42 (Database issue), D643–D648. https://doi.org/10.1093/nar/gkt1209

Yu T-L, Wang B-S, Shen C-C, Wang P-L, Yang TF, Burr GS & Chen Y-G (2017). Improved analytical techniques of sulfur isotopic composition in nanomole quantities by MC-ICP-MS. Analytica Chimica Acta, 988,34-40.

Zhang, J., Shi, Q., Fan, S., Zhang, Y., Zhang, M., & Zhang, J. (2021). Distinction between Cr and other heavy–metal–resistant bacteria involved in C/N cycling in contaminated soils of copper producing sites. Journal of Hazardous Materials, 402, 123454. https://doi.org/10.1016/J.JHAZMAT.2020.123454

Åberg, A. K., Korkka-Niemi, K., Åberg, S. C., & Rautio, A. (2025). Application of 3D hydrogeochemistry and particle tracking in detecting groundwater flow patterns within an aapa mire–outwash plain system in a boreal environment at a mining development site. Applied Geochemistry, 186, 106360. https://doi.org/10.1016/J.APGEOCHEM.2025.106360

Åberg, A.K., Putkinen, N., Eyles, N., Davidila, J., and Malinowski, M. (2026). 3D hydrostratigraphic architecture of a Late Pleistocene buried valley infill at Kurikka, west-central Finland. Quaternary International 755:110080. https://doi.org/10.1016/j.quaint.2025.110080

Åkesson, M., Suckow, A., Visser, A., et al. (2015). Constraining age distributions of groundwater from public supply wells in diverse hydrogeological settings in Scania, Sweden. J Hydrol 528:217–229. https://doi.org/10.1016/j.jhydrol.2015.06.022